AD-A036 310 STANFORD RESEARCH INST MENLO PARK CALIF F/G 17/2.1
IONOSPHERIC EFFECTS ON RADIO PROPAGATION. A SUMMARY AND SELECTE--ETC(U)
SEP 76 W W BERNING DNA001-74-C-0167
UNCLASSIFIED DNA-4119T NL

| OF |
AD
A036310

END

DATE
FILMED
3-77

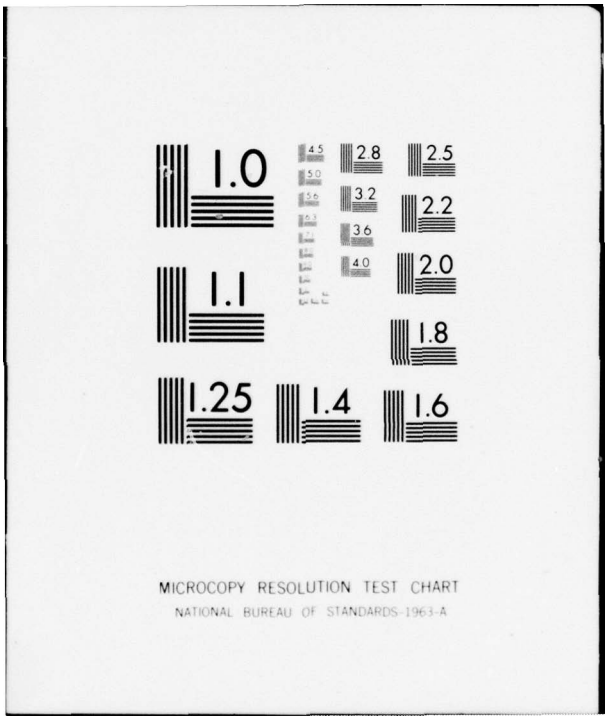
1.0
1.1
1.25
1.4
1.6
1.8
2.0
2.2
2.5
2.8
3.2
3.6
4.0
4.5
5.0
5.6
MICROCOPY RESOLUTION TEST CHART
NATIONAL BUREAU OF STANDARDS-1963-A

(19) (18) DNA 4119T (12)

IONOSPHERIC EFFECTS ON RADIO PROPAGATION.

A Summary and Selected Analysis of Ionospheric Measurements in the Rocket and Satellite Tracking Programs of the U.S. Army Ballistic Research Laboratories.

Stanford Research Institute
333 Ravenswood Avenue
Menlo Park, California 94025

(11) September 1976 (12) 56 p.

(9) Topical Report

(15) CONTRACT No. DNA 001-74-C-0167

(10) Warren W. Berning

THIS WORK SPONSORED BY THE U.S. ARMY BALLISTIC RESEARCH LABORATORIES MIPR 647-76 TO THE DEFENSE NUCLEAR AGENCY AND PREPARED UNDER CONTRACT NO. DNA 001-74-C-0167, TASK AND SUBTASK Q79AAXHX631, WORK UNIT 01.

Prepared for

Director
DEFENSE NUCLEAR AGENCY
Washington, D. C. 20305

Destroy this report when it is no longer needed. Do not return to sender.

UNCLASSIFIED

SECURITY CLASSIFICATION OF THIS PAGE *(When Data Entered)*

REPORT DOCUMENTATION PAGE		READ INSTRUCTIONS BEFORE COMPLETING FORM
1. REPORT NUMBER DNA 4119T	2. GOVT ACCESSION NO.	3. RECIPIENT'S CATALOG NUMBER
4. TITLE *(and Subtitle)* IONOSPHERIC EFFECTS ON RADIO PROPAGATION		5. TYPE OF REPORT & PERIOD COVERED Topical Report
		6. PERFORMING ORG. REPORT NUMBER Project No. 3118
7. AUTHOR(s) Warren W. Berning		8. CONTRACT OR GRANT NUMBER(s) DNA 001-74-C-0167
9. PERFORMING ORGANIZATION NAME AND ADDRESS Stanford Research Institute 333 Ravenswood Avenue Menlo Park, California 94025		10. PROGRAM ELEMENT, PROJECT, TASK AREA & WORK UNIT NUMBERS Subtask Q79AAXHX631-01
11. CONTROLLING OFFICE NAME AND ADDRESS U.S. Army Ballistic Research Laboratories Aberdeen Proving Ground, Maryland 21005		12. REPORT DATE September 1976
		13. NUMBER OF PAGES 58
14. MONITORING AGENCY NAME & ADDRESS *(if different from Controlling Office)* Director Defense Nuclear Agency Washington, D.C. 20305		15. SECURITY CLASS *(of this report)* UNCLASSIFIED
		15a. DECLASSIFICATION/DOWNGRADING SCHEDULE

16. DISTRIBUTION STATEMENT *(of this Report)*

Approved for public release; distribution unlimited.

17. DISTRIBUTION STATEMENT *(of the abstract entered in Block 20, if different from Report)*

18. SUPPLEMENTARY NOTES

This work sponsored by the U.S. Army Ballistic Research Laboratories MIPR 647-76 to the Defense Nuclear Agency and prepared under Contract No. DNA 001-74-C-0167, Task and Subtask Q79AAXHX631, Work Unit 01.

19. KEY WORDS *(Continue on reverse side if necessary and identify by block number)*

Ionosphere
Auroral Ionosphere
Ionospheric Propagation
Guided Missile Tracking System

20. ABSTRACT *(Continue on reverse side if necessary and identify by block number)*

This report is intended to be a very brief survey of work carried out by the U.S. Army Ballistic Research Laboratories in that portion of their upper atmosphere research program concerned with ionospheric effects on radio propagation. Preparation of this survey has been supported entirely by the Ballistic Research Laboratories through a Military Interdepartmental Procurement Request to the Defense Nuclear Agency. The large majority of work summarized herein has been reported in BRL Reports and Memorandum Reports.

DD FORM 1 JAN 73 1473 EDITION OF 1 NOV 65 IS OBSOLETE

UNCLASSIFIED

SECURITY CLASSIFICATION OF THIS PAGE *(When Data Entered)*

4. TITLE (and Subtitle) (Continued)

A Summary and Selected Analysis of Ionospheric Measurements in the Rocket and Satellite Tracking Programs of the U.S. Army Ballistic Research Laboratories

20. ABSTRACT (Continued)

The thrust of this present effort has been the extraction and discussion of ionospheric effects on radio propagation which continue to be of importance in the performance and effectiveness of communications systems.

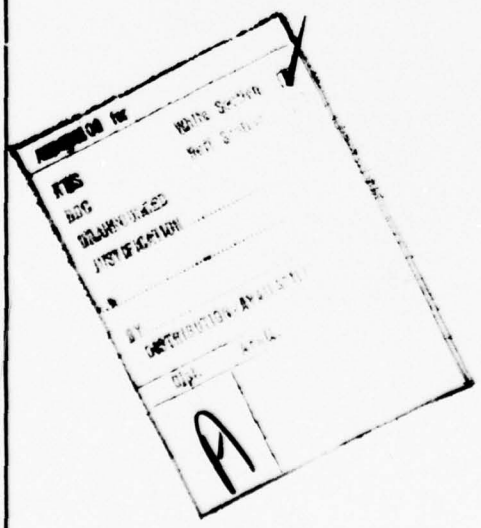

PREFACE

This report is intended to be a very brief survey of work carried out by the U.S. Army Ballistic Research Laboratories in that portion of their upper atmosphere research program concerned with ionospheric effects on radio propagation. Preparation of this survey has been supported entirely by the Ballistic Research Laboratories under Department of Army Project DA12161-102-B53A through a Military Interdepartmental Procurement Request to the Defense Nuclear Agency. The large majority of work summarized herein has been reported in BRL Reports and Memorandum Reports. The thrust of this present effort has been the extraction and discussion of ionospheric effects on radio propagation which continue to be of importance in the performance and effectiveness of communications systems.

TABLE OF CONTENTS

PREFACE		1
I	INTRODUCTION	5
II	METHODS EMPLOYED	12
	A. Trajectory Comparison Method.	12
	B. Faraday Rotation.	15
	C. Dispersive Doppler.	17
	D. Signal Attenuation.	19
III	PROPAGATION EFFECTS.	21
	A. Ionospheric Tilts	21
	B. Radio Signal Absorption	22
	C. Signal Refraction	24
	D. Focusing, Defocusing, Multipath and Diffraction	26
IV	EXAMPLE SELECTED FOR ANALYSIS.	33
	Focusing and Defocusing of Signals	33
V	SUMMARY AND CONCLUSIONS.	48
BIBLIOGRAPHY.		49

LIST OF ILLUSTRATIONS

Figure 2.1 SCHEMATIC OF RADIO TRACKING SYSTEM 13
Figure 2.2 ELECTRON DENSITIES FROM TRAJECTORY COMPARISON METHOD 16
Figure 2.3 EFFECT OF FARADAY ROTATION ON SPIN CORRECTIONS APPLIED TO DOVAP REDUCTIONS. 18
Figure 3.1 IONOSPHERIC ELECTRON CONTENT SHOWING STRONG HORIZONTAL GRADIENT. 23
Figure 3.2 RF ABSORPTION FOR ROCKET B-6 25
Figure 3.3 SKETCH ILLUSTRATING THE EFFECT OF AN IONIZED CLOUD ON PROPAGATION PATHS 27
Figure 3.4 SIGNAL LEVEL OF 72MHz TRANSMISSION RECEIVED AT WALLOPS ISLAND LAUNCH SITE. PROJECT HAVEN BARTER . . 28
Figure 3.5 291/874 MHz DISPERSIVE PHASE VERSUS TIME FOR THE PLUM CLOUD 31
Figure 3.6 ELECTRON CONCENTRATION IN A SLICE THROUGH THE PLUM CLOUD MODEL, PERPENDICULAR TO THE MAGNETIC FIELD, AT 120 AND 150 SECONDS AFTER RELEASE 32
Figure 4.1 PLASMA SPHERE REFRACTION 39
Figure 4.2 ATTENUATION FROM SIGNAL DEFOCUSING 40
Figure 4.3 RADIO FREQUENCY ATTENUATION ILLUSTRATING FOCUS/DEFOCUS. 41
Figure 4.4 PCA-69 ELECTRON DENSITY PROFILES 42
Figure 4.5 FLIGHT SCHEMATIC, ROCKET B-2 44
Figure 4.6 RAY PATHS THROUGH POSTULATED DISTURBANCE 46

LIST OF TABLES

Table 1.1 BRL IONOSPHERIC MEASUREMENTS DURING COORDINATED GEOPHYSICAL STUDIES IN THE INTERNATIONAL GEOPHYSICAL YEAR 8

Table 1.2 BRL IONOSPHERIC MEASUREMENTS DURING COORDINATED GEOPHYSICAL STUDIES IN THE POLAR CAP ABSORPTION EVENT OF 1969. 9

Table 1.3 BRL IONOSPHERIC MEASUREMENTS DURING BARIUM PLASMA RELEASE EXPERIMENTS, SECEDE II AND SECEDE III. . . . 10

Table 4.1 MEASURED vs PREDICTED MAXIMUM ATTENUATION, HAVEN BARTER RELEASE NO. 2 37

I INTRODUCTION

In the years 1948-71, the Ballistic Research Laboratories (BRL) developed several methods for the study of ionospheric characteristics with the principal objective of understanding the effects of the ionosphere, disturbed and undisturbed, upon the propagation of radio signals used for the tracking of objects emitting signals and in the transmission of information. The major efforts focused on the use of radio methods for the diagnostic studies in the belief that the most direct access to propagation effects could thereby be obtained. This approach of necessity led to inferential determination of ionospheric characteristics through the postulation of simple or complex models of ionospheric structure followed by iterative modifications of the models to provide compatibility between predicted and observed propagation effects. Sensitivity of the method was provided through use of multiple coherent frequencies, careful attention to antenna and polarization properties of the equipments and sophisticated detection and recording of the received signals.

The earliest efforts of the BRL to assess the effects of the ionosphere on radio signals were associated with the mission of developing, installing and operating the missile tracking system known as Doppler Velocity and Position (DOVAP) at the White Sands Missile Range in the late 1940s. This system, which will be described briefly in a following section, was capable of real-world tracking accuracies equivalent to the best of the ballistic cameras and was not equaled in accuracy by microwave systems until the advent of sophisticated phased-array radars in the late 1960s. A precursor to the DOVAP system was developed in Germany in the early 1940s to provide accurate velocity information for long range ballistic rockets (V-2) since radar in those years was incapable of providing the needed data. With the DOVAP system, basic trajectory information is derived by measuring, at the ground, the phase of radio signals transmitted to and from the object being tracked. Distances, then, are related to

phase through the transmitted frequency and velocity of propagation (phase velocity). The phase velocity of propagation in the ionosphere is greater than the vacuum velocity of light so that DOVAP range information is foreshortened with respect to true values for objects tracked in and above the ionosphere. For the DOVAP system operating at White Sands Missile Range with frequencies of 37 and 74 MHz, the range error could be as much as 2 kilometers at an altitude of 1,000 kilometers. Efforts at the BRL were directed to finding ionosphere corrections for the DOVAP data; by a modeling process, these corrections could be used to describe the altitude profile of total electron content in the ionosphere.[1] The same basic method, but with much improved data handling and analysis, was developed for determining the ionospheric structures of Mars and Venus during the Mariner missions.[2 3 4 5]

In the late 1950s, the two-frequency method of determining ionospheric properties, developed first by Seddon,[6] was adopted by the BRL to enable more accurate measurements of ionospheric properties and to free such measurements from restriction to launch facilities equipped with the DOVAP tracking system. The BRL utilized frequencies of 36/145 MHz for the two-frequency experiment because of long familiarity with appropriate equipments, because data from frequencies below approximately 20 MHz become increasingly difficult to interpret, because rocket antennas are relatively easy to design for such frequencies, and because of minimum background interference. This adopted method was applied in a series of experiments, identified as STRONGARM, carried out at Wallops Island, Va., in 1959-60.[7] Shortly after these experiments, a crash effort was initiated to prepare and field rocket-borne multi-frequency beacons for the high altitude nuclear tests at Johnston Island in 1962.[8] For this program, a third coherent frequency at 888 MHz was added to provide greater dynamic range in the measurements taken. Eighteen rockets equipped with these multi-frequency beacons were flown during the test program.

---

* The frequencies noted throughout this report are rounded to the nearest MHz. Where frequency ratios are given, such frequencies are phase-coherent.

Following the nuclear tests at Johnston Island, the BRL participated in the Test Readiness Program called for under Safeguard C of the Limited Test Ban Treaty. Supported by this program, the multi-frequency propagation experiment was greatly improved in ground instrumentation, data processing and analysis, antenna design, and rocket-borne transmitting equipment. Eventually, five coherent frequencies were incorporated into the experiment design covering the range 36-875 MHz. Under the Test Readiness Program, the BRL propagation experiment was brought to a high degree of perfection.

In the years after 1962, ionospheric measurements by the BRL were always carried out in support of field programs whose objectives were substantially broader than the isolated measurement of ionospheric parameters. Thus, the BRL provided ionospheric data for the barium release programs SECEDE II and SECEDE III[9] [10] and the coordinated geophysical studies in the polar cap absorption (PCA) event in November 1969.[11] [12] All the high altitude rocket experiments carried out by the BRL have been catalogued;[13] however, the more significant data samples of ionospheric electron content and densities from rocket experiments are listed in Tables 1.1, 1.2, and 1.3. In time, data taken in the auroral regions at times of sunspot maximum (including the data in Tables 1.1 and 1.2) may become increasingly important if sunspot activity is entering a declining phase. Certainly solar activity in the 1968-69 period of sunspot maximum was considerably less than the 1957-58 period, and it has been noted recently that the 11-year solar cycle may not be a constant characteristic of the sun and solar activity has been very small for long periods of time in the past.[14] Thus, design of communications systems for the relatively benign radio transmission environment accompanying times of low sunspot activity could yield marginal or disrupted performance in the more vigorous ionospheric environment created by solar or man-made disturbances in the high atmosphere.

In the late 1950s, the BRL, as well as others, became interested in the use of satellites as carriers for radio transmitters and the promise of a major new capability for ionospheric studies using signals from such

Table 1.1

BRL IONOSPHERIC MEASUREMENTS DURING COORDINATED GEOPHYSICAL STUDIES IN THE INTERNATIONAL GEOPHYSICAL YEAR

Date	Time (CST)[1]	Location	Data Type[2]	Altitude Interval[3]	Remarks
1956					
20 Oct.	1601	Ft.Churchill,Canada	[1]	95-109	
23 Oct.	0240	Ft.Churchill,Canada	[1]	95-130	
1957					
4 July	1216	Ft.Churchill,Canada	[1][2][3]	100-235	Also carried Seddon 2-freq. experiment
29 July	1600	Ft.Churchill,Canada	[2]	100-210	
1958					
25 Jan.	2219	Ft.Churchill,Canada	[1][2]	120-180	Launched into visible aurora; ionosphere not highly disturbed
3 Feb.	1202	Ft.Churchill,Canada	[1][2][3]	100-138	
4 Feb.	0017	Ft.Churchill,Canada	[1][2]	100-230	Large spatial variations in ionization
24 Feb.	0100	Ft.Churchill,Canada	[1][2]	110-200	
24 Feb.	0135	Ft.Churchill,Canada	[2]	90-145	Extremely low electron content ($<10^{15}$ m^{-2} column)
20 Oct.	1601	Ft.Churchill,Canada	[1][3]	95-130	
31 Oct.	1359	Ft.Churchill,Canada	[1][2][3]	90-190	
7 Nov.	1953	Ft.Churchill,Canada	[1][3]	90-135	
13 Nov.	0259	Ft.Churchill,Canada	[1]	95-140	
24 Nov.	0025	Ft.Churchill,Canada	[2]	95-205	Highly disturbed ionosphere; visible aurora not exceptional. Electron content can only be approximated.
30 Nov.	1237	Ft.Churchill,Canada	[1][2][3]	130-280	

[1] Times given in U.T. would read 6 hours later.

[2] Data Type: [1] Total Electron Content, Trajectory Comparison; [2] Total Content, Faraday Rotation; [3] Inferred Electron Densities.

[3] Altitude interval (kilometers) within which data were obtained.

Table 1.2

BRL IONOSPHERIC MEASUREMENTS DURING COORDINATED GEOPHYSICAL STUDIES IN THE POLAR CAP ABSORPTION EVENT OF 1969

Date (1969)	Time (CST)[1]	Location	Data Type[2]	Altitude Interval[3]	Remarks
2 Nov.	1510 (B-4)[4]	Ft. Churchill, Canada	[1][2][3]	45-119	Attenuation at 9, 18 and 36 MHz. Carried Langmuir Probe
3 Nov.	0657 (B-2)	Ft. Churchill, Canada	[1][2][3]	65-118	Attenuation at 36 and 145 MHz.
3 Nov.	0730 (B-3)	Ft. Churchill, Canada	[1][2][3]	60-112	Attenuation at 9, 18 and 36 MHz
3 Nov.	1254 (B-5)	Ft. Churchill, Canada	[1][2][3]	55-125	Attenuation at 9, 18 and 36 MHz. Carried Langmuir Probe
4 Nov.	1530 (B-6)	Ft. Churchill, Canada	[1][2][3]	55-125	Attenuation at 9, 18 and 36 MHz. Carried Langmuir Probe
4 Nov.	1638 (B-7)	Ft. Churchill, Canada	[1][2][3]	60-125	Attenuation at 18 and 36 MHz. Carried Langmuir Probe

[1] Add 6 hours for Universal Time (UT).

[2] Data type: [1] Total Electron Content; [2] Inferred Electron Densities; [3] Signal attenuation. Electron content (and inferred electron density) from 36/145/583 MHz phase-coherent transmitter.

[3] Altitude interval (kilometers) within which data were obtained.

[4] Flight identification numbers.

Table 1.3

BRL IONOSPHERIC MEASUREMENTS DURING BARIUM PLASMA RELEASE EXPERIMENTS, SECEDE II AND SECEDE III

Date	Time (UT)	Location	Data Type[1]	Altitude Interval[2]	Remarks[3]
			SECEDE III, 1969		
6 March	0430	Fairbanks, Alaska	[1][2]	80-170	
11 March	1408	Fairbanks, Alaska	[1][2]	85-170	Electron content almost 10 times that of 5 March experiment
15 March	0506	Fairbanks, Alaska	[1][2]	85-210	Smooth ionosphere profile but large magnetic field disturbance
19 March	0517	Fairbanks, Alaska	[1][2]	75-220	
20 March	0537	Fairbanks, Alaska	[1][2]	90-175	
			SECEDE II, 1971		
20 Jan.	2346	Eglin AFB, Florida	[1][2]	90-240	Two marked sporadic E layers
26 Jan.	2350	Eglin AFB, Florida	[1][2]	140-300	
29 Jan.	2352	Eglin AFB, Florida	[1][2]	130-250	Sporadic E, approximately 140 km.
30 Jan.	0024	Eglin AFB, Florida	[1][2]	95-260	Two layers of sporadic E at 110 and 125 km.
2 Feb.	0001	Eglin AFB, Florida	[1][2]	90-250	Sporadic E at 110 km.
2 Feb.	1632	Eglin AFB, Florida	[1][2]	90-260	

[1] Data Type: [1] Total Electron Content; [2] Inferred Electron Densities.

[2] Altitude interval (kilometers) within which data were obtained.

[3] SECEDE III measurements employed a 36/145/583 MHz phase-coherent beacon. SECEDE II used 36/145/292/437/875 MHz beacon.

transmitters. When the Sputnik I was launched, the BRL had designed and was already assembling ground receiving equipments for use with satellite transmitters and was quickly able to initiate tracking of Sputnik. This early experience made possible a rapid development of data reduction methods and analysis, and incorporation of the necessary receivers and antennas in the ground station used for the multi-frequency rocket experiments. Thus, ionospheric measurements could be made as soon as the two-frequency navy navigation satellites, launched under the Transit Program, were placed in orbit. When the U.S. high altitude nuclear tests were carried out in the Pacific in 1962, it was possible to measure total electron content in the ionosphere (below approximately 900 kilometers) for 95 passes of Transit 4A and Transit 4B (Omicron 1 and Alpha Eta 1) in the period 17 May through 4 November 1962. The ground tracking station was located at Johnston Island and data were obtained at latitudes of 5-25 degrees north and longitudes of 160-180 degrees west.[8 15] The methods developed at the BRL and by other investigators made possible ionosphere corrections to position and velocity information for the many users of the Transit navigation system.

For a variety of reasons, a major one being changing roles and missions, BRL activities in rocket measurements in the upper atmosphere were phased out rather quickly after 1971. The major contribution of the high altitude rocket measurements and satellite tracking programs of the BRL was the development and perfection of methods for analyzing and understanding the transmission of phase-coherent, multi-frequency signals through disturbed ionospheres.

II METHODS EMPLOYED

As mentioned in the previous section, the thrust of BRL efforts to determine ionospheric effects on radio signals changed from an emphasis on correcting radio tracking data to the use of radio signals for diagnostic measurements of disturbed ionospheres. This changing emphasis, together with rapidly improving electronic and recording equipments, led to evolutionary changes in instrumentation as well. The result was a better capability to assess ionospheric effects and provide a base of information to predict these effects for a variety of ionospheric structures and other frequency regimes.

In this section, the methods used by the BRL in assessing ionospheric effects on radio signals are briefly reviewed; more detailed discussions are found in various BRL reports.[15 16 17 18]

A. Trajectory Comparison Method

As mentioned in the previous section, the earliest BRL efforts in investigation of ionospheric effects were associated with the operation of the DOVAP missile tracking system at the White Sands Missile range. The ionospheric effects associated with the phase comparison tracking system were later used for inferential determination of ionospheric structures of Mars and Venus.[2 3 5]

A portion of the DOVAP tracking system is represented schematically in Figure 2.1. In operation, a radio signal from the transmitter is received by the missile, doubled in frequency and retransmitted to three or more ground receivers. The same transmitter signal is sent by ground link to the same receiver sites, doubled in frequency and mixed with the signals received via the rocket transmitter. Because phase coherence is retained throughout the system, the resultant total signal phase, after mixing and

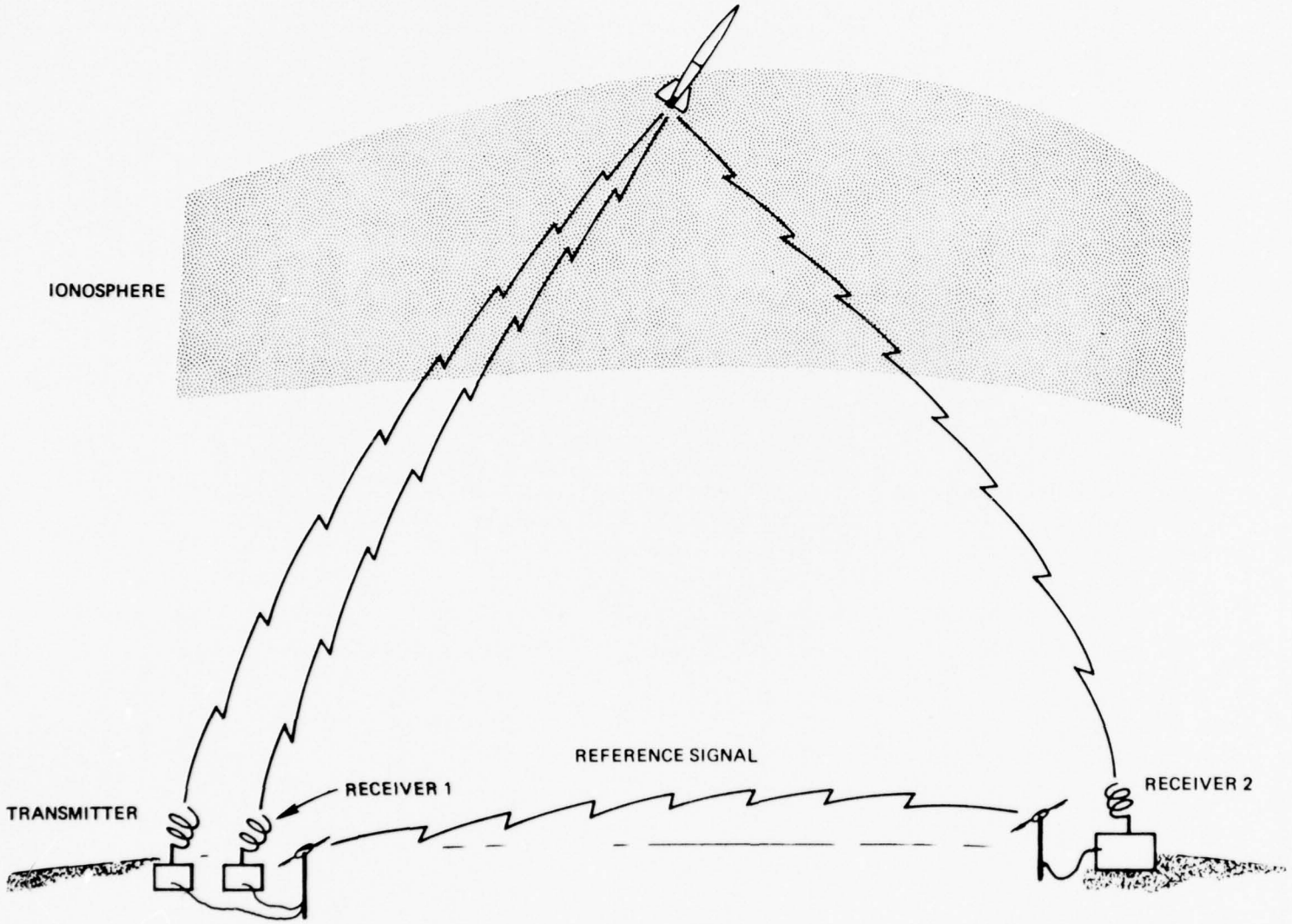

Figure 2.1 SCHEMATIC OF RADIO TRACKING SYSTEM

multiplication by the wavelength of the doubled frequency, provides a measure of the distance from the transmitter-to rocket-to ground receiver. Knowledge of the total phase requires continuous recording of the mixed signals from the time of missile lift-off. For the general case of non-coincident transmitter and receiver, the measured distance generates an ellipsoid of revolution. The intersection of three such ellipsoids (requiring three receivers) locates the missile in space. For the special case of coincident transmitter and receiver, the ellipsoid becomes a sphere.

Because rocket-borne antennas frequently have dipole patterns, ground antennas have circular, or quasi-circular, polarization to avoid signal dropouts and abrupt phase shifts. As a consequence, the phase of received signals is affected by missile spin and polarization rotation arising from the Faraday effect (earth's magnetic field interaction with the electric field of the radio signals). Accordingly, reduction of measured phase accumulation to determine missile position must consider all phase changes arising from E-vector rotation.

In the reduction of phase data acquired by the DOVAP system, the assumption is made that the wavelength used in converting phase to distance is that appropriate to signal propagation in vacuo, ie., $\lambda f = C_o$ where λ and f are the wavelength and frequency of the tracking signal used, and C_o is the vacuum speed of light. In fact, however, in a dispersive medium such as the ionosphere, the propagation speed is not C_o; for a phase-measuring system the phase velocity of propagation in the ionosphere is greater than C_o. Thus, the range measurements, S_D, derived in the DOVAP system are given by the relation, $S_D = \phi_D C_o / f$ (where ϕ_D is the measured total phase at any point in the trajectory) when in fact the true range, S, is given by, $S = \phi_D C / f$, with C being the correct value for propagation speed in the dispersive medium. The relationship of C to the various parameters describing the ionosphere (electron and ion densities, collision frequencies, electron and ion gyrofrequencies, etc.) has been known for many years and discussed extensively.[19] If the basic system frequency is sufficiently high, the true speed of propagation is almost entirely a function of the free electron

density in the ionosphere and can be expressed by a very simple relationship. Further, for sufficiently high frequencies, the assumption of straight-line propagation in the ionosphere introduces negligible error in derived trajectory parameters. If the ionosphere has horizontal uniformity in the space occupied by the missile and the tracking system, differences in S_D and S can be related simply to altitude differences, h_D and h. Thus, a measurement of the quantities S_D and S, together with a simple expression relating their difference to ionospheric electron density, makes possible, through an inversion process, the measurement of electron content in the ionosphere below the altitude of a tracked missile.

In the absence of an independent range measuring system, unaffected by the ionosphere, the quantities S or h are not directly available. However, the DOVAP system is sufficiently accurate that a vacuum trajectory (or orbit) may be computed using initial conditions from the DOVAP trajectory after missile burnout and above the effective drag region but before the missile enters the ionosphere. The quantities S or h are given by the vacuum trajectory parameters. In Figure 2.2 is shown a typical profile of electron density versus altitude derived through application of the method described. The error bars are representative of the accuracy of this method. Accuracies are poor for small electron densities and small missile speeds.

B. Faraday Rotation

Because of the earth's magnetic field, the ionosphere is birefringent so that a linearly polarized wave propagating through the ionosphere is broken into two counter-rotating circularly polarized waves traveling at slightly different velocities. These are familiarly known as the ordinary and extra-ordinary waves. The combination of these two waves, as seen by an antenna, as the waves propagate would appear to be a linearly polarized wave whose plane of polarization is slowly rotating. This rotation is called Faraday rotation after its discoverer. The same phenomenon occurs for circularly polarized waves as well. In effect, the Faraday rotation advances or retards the rotating vector as the wave proceeds.[22]

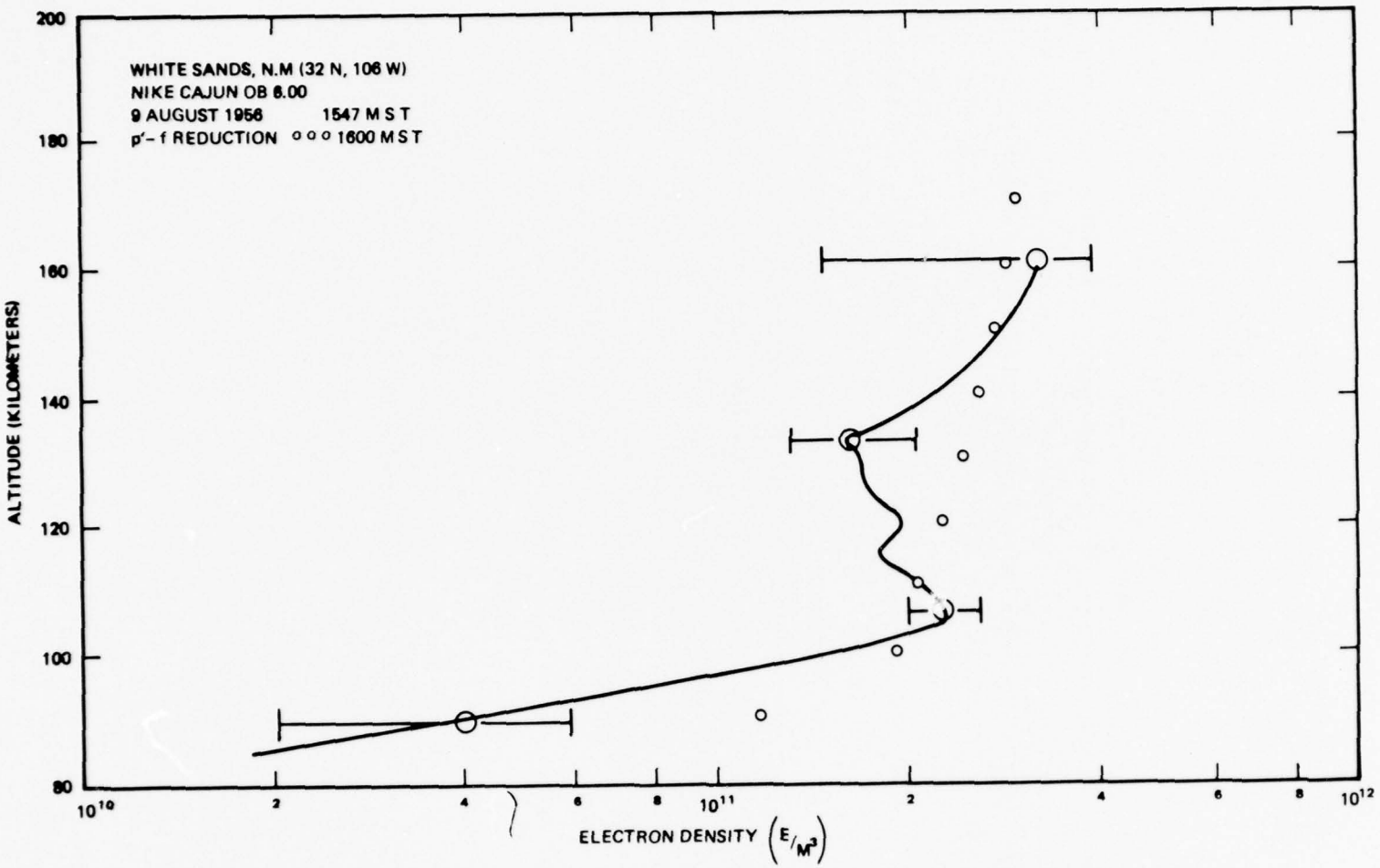

Figure 2.2 ELECTRON DENSITIES FROM TRAJECTORY COMPARISON METHOD

3

As mentioned earlier, missile spin and Faraday rotation introduce phase contributions to the total measured phase, ϕ_D, which must be removed in providing accurate trajectory information. To provide the needed corrections, each receiver site acquires phase data through two oppositely circularly polarized antennas. Mixing of the signals received through the two antennas provides phase data proportional to polarization rotation resulting from the sum of missile spin and Faraday rotation. This phase information permits the necessary corrections for accurate trajectory determination. Through a simple analytical procedure it is possible to separate the missile spin and Faraday contributions to the total E-vector rotation.[18] In fashion analogous to the trajectory comparison technique, missile spin is determined above the altitude of appreciable drag but prior to missile entry into the ionosphere. Figure 2.3 illustrates the method of determining Faraday rotation information from the recorded DOVAP spin data. For frequencies used in the trajectory comparison method, Faraday rotation is proportional to the total electron content between the missile and ground receivers. Determination of electron content from Faraday rotation data is less accurate than information from trajectory comparison; however, the data are relatively easy to obtain.

C. Dispersive Doppler

Referring to Figure 2.1, it is clear that if the information desired is the structure of the ionosphere, the transmission of two or more frequency-coherent signals from the missile will provide data more simply and accurately than the trajectory comparison method. Choosing a relatively large frequency ratio (although this is certainly not necessary) and the lowest frequency such that differences in ray paths can be ignored, dispersive or differential phase differences are readily obtained by mixing the signals received at the ground, after suitable multiplication of the lower frequency by the frequency ratio. This dispersive phase can be readily related to ionospheric parameters and the techniques have been extensively discussed.[6 16 17 28] All BRL activities after 1958 related to ionospheric propagation measurements employed the dispersive doppler or differential phase technique.

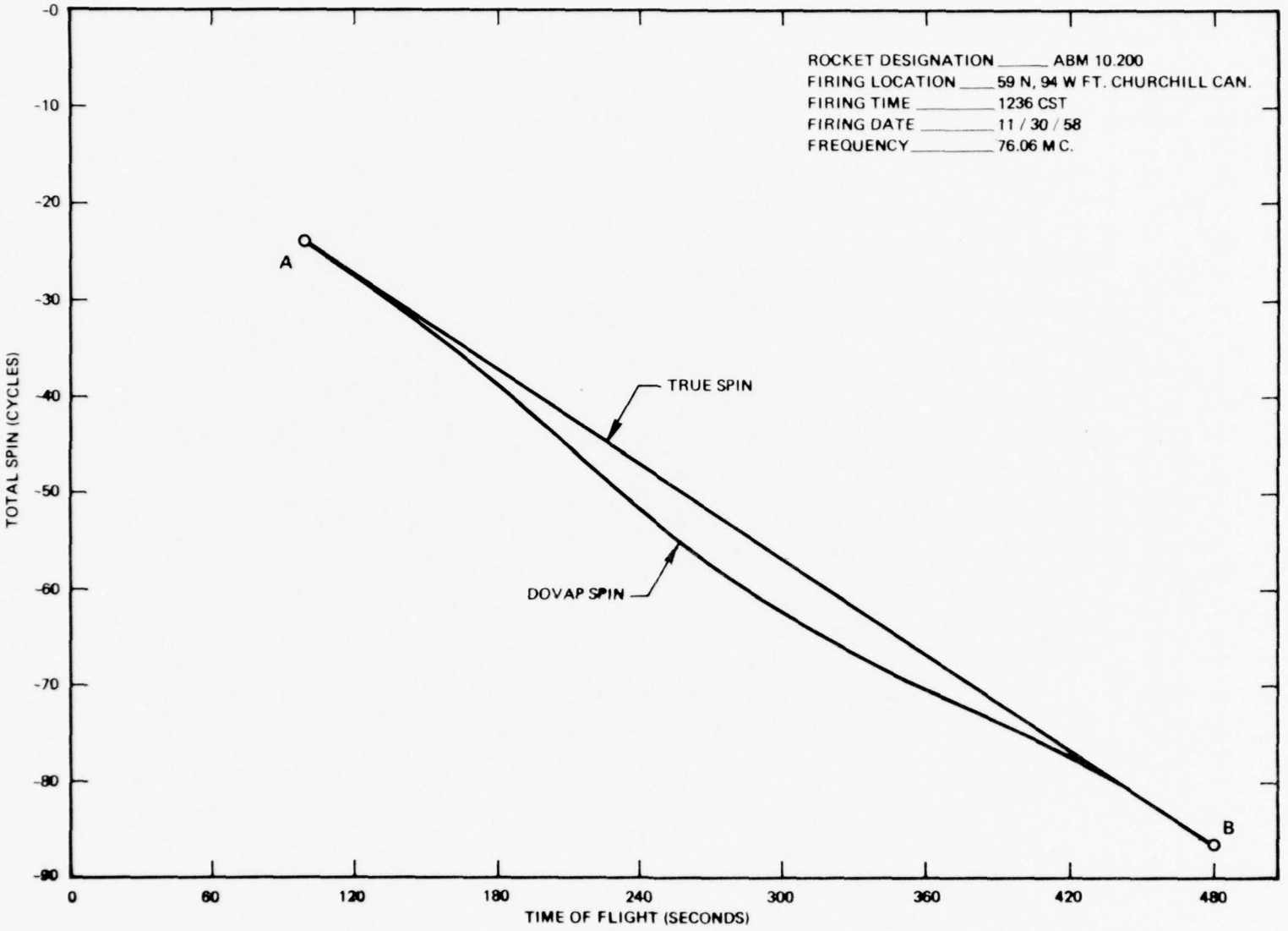

Figure 2.3 EFFECT OF FARADAY ROTATION ON SPIN CORRECTIONS APPLIED TO DOVAP REDUCTIONS

Ionospheric measurements using the techniques of Faraday rotation and dispersive doppler have been obtained with signals transmitted by satellites. For satellites, it is not easily possible to maintain continuous signal reception from lift-off of the satellite so that a phase ambiguity of many cycles exists in the dispersive doppler or Faraday rotation data for any given pass of the satellite over a ground receiving station. For the case of Faraday rotation, the ambiguity may be removed in theory for a given satellite pass if signal propagation normal to the earth's magnetic field occurs sometime during that pass. For such a condition, the Faraday rotation is zero so that accumulated Faraday cycles can be determined by counting forward and backward from the normality condition. In practice, however, the propagation vector is not normal to the earth's field along the entire propagation path so at best a rather fuzzy region occurs in a portion of track where the ray path is close to the perpendicular configuration; and the ambiguity is not easily resolved. If, however, dispersive doppler and Faraday rotation are recorded simultaneously, it is possible, by a hybrid method, to remove the ambiguity and derive data for total electron content below the satellite altitude.[15 20 21] The hybrid technique was used to develop an extensive data set during the high altitude nuclear tests in 1962, referred to earlier in Section I (and see Figure 3.1).

D. Signal Attenuation

As a general statement, signal attenuation derives from several distinct mechanisms. The familiar and rather obvious mechanism is that of spherical expansion of a transmitted wave, with the energy, or power, decreasing as the inverse square of the distance from the transmitter. Almost as familiar as spherical expansion is the absorption of signal energy through the collision of electrons or ions with each other or with the neutral constituents in the atmosphere during passage of the signal. The equations which govern absorption are well known.[19] This does not imply that the atmospheric parameters are sufficiently well known that absorption can be confidently predicted in all frequency regimes or for all levels of atmospheric disturbance. The third source of attenuation arises from

a variety of propagation conditions which may amplitude- and phase-modulate the passing signals (e.g., diffraction and multipath) or for which the radius of curvature of an expanding wave front is markedly changed (e.g., focusing and defocusing). This last source of attenuation will be discussed more fully in the following sections.

Signal attenuation arising from the absorption of energy is very important for significant portions of the radio spectrum (HF frequencies and below in the ionized atmosphere, X-band and above in the non-ionized atmosphere). The method employed by the BRL was quite straight-forward. The zero-absorption level was defined as the signal level (properly corrected for antenna pattern effects) at the points of entry into and exit from the ionosphere. A straight line joining these points, in a plot of signal level (db below one milliwatt) as a function of slant range, established the zero absorption signal level during the time the tracked vehicle was in or above the ionosphere. Signal level departures from this straight line interpolation were attributed to absorption of the signal energy. An example of measured absorption derived by this method is shown in Figure 3.2, where slant range has been converted to altitude of the vehicle being tracked.

III PROPAGATION EFFECTS

In the previous sections, reference was made to effects of the ionosphere on a particular radio tracking system (DOVAP) used for trajectory determinations. In point of fact there are ionospheric effects on such systems which were not described; such effects are important for a much broader family of radio systems used for communications purposes. Further, ionospheric effects are important for radio navigation systems and the greater the demand for system accuracy, the more important becomes the knowledge of propagation factors required for ionospheric compensation. The basic methods described in Section II are those used today, but with major improvements in precision, accuracy and data handling capability. In this section, several propagation effects not addressed or addressed briefly in previous sections will be discussed.

A. Ionospheric Tilts

For purposes of determining propagation effects in the various radio-frequency systems, the ionosphere is frequently assumed to be horizontally stratified. Although such an assumption simplifies calculations and expressions for propagation path refraction, marked horizontal gradients in ionization occur on occasion everywhere on earth and very frequently for a large portion of the ionosphere. The so-called ionospheric "tilts" make difficult the prediction of usable frequencies for given point-to-point communications at high frequency (HF), are responsible for anomalous HF propagation, and give rise to the phase and amplitude variations of importance for VLF and ELF communications systems. In recent years, the burden of radio communications has shifted to higher capacity, higher frequency systems, but abundant interest remains in high frequency communications on the part of many present and potential subscribers. Ionospheric tilts can enhance as well as degrade the range of HF systems, and can give rise to the irritating condition of non-reciprocal communications.

An example of a marked ionospheric tilt is shown in Figure 3.1. The data were obtained in 1962 from the tracking of Transit satellites using the hybrid Faraday-Doppler technique.[15] A twofold increase in total electron content occurred between the north latitudes of 18^{o}-22^{o}, or west longitudes of 163^{o}-155^{o}, or some combination of both. At the local time of satellite passage, gradients in the west-east direction are normally small and the observed gradient is probably indicative of a strong south-to-north increase in content. In the summer northern hemisphere, a maximum in electron content usually occurs between 15^{o}-25^{o}, arising, most likely, from subsidence of ionized constituents convected to high altitudes by $\vec{E} \times \vec{B}$ drift in the equatorial electrojet. The data shown in Figure 3.1 indicate a higher-than-usual maximum electron content. From the standpoint of HF propagation, the electron content profile shown would indicate a substantial ionospheric tilt and a difficult situation for establishing a north-south communications link.

B. Radio Signal Absorption

In the previous section, sources of signal attenuation in the ionosphere were briefly summarized. The absorption of signal energy occurs under conditions when the signal frequencies are of the same order as the collision frequencies of the ionized particles with the neutral atmospheric particles, and with each other. Absorption also occurs when the signal frequency approaches the plasma frequency of the ionized medium. For the latter case, however, ionization gradients become very important because refraction of the signals becomes very large and the signals are essentially reflected away from the strongly absorbing regions. Thus, VLF and ELF are trapped in the so-called ionospheric waveguide with relatively little energy removed by electron collisions.

For HF, and for lower frequencies as well, electron collisions can remove substantial energy, and absorption is an important consideration when appreciable ionization exists at altitudes where electron collision frequencies approach signal frequencies. In disturbed ionospheres, in particular

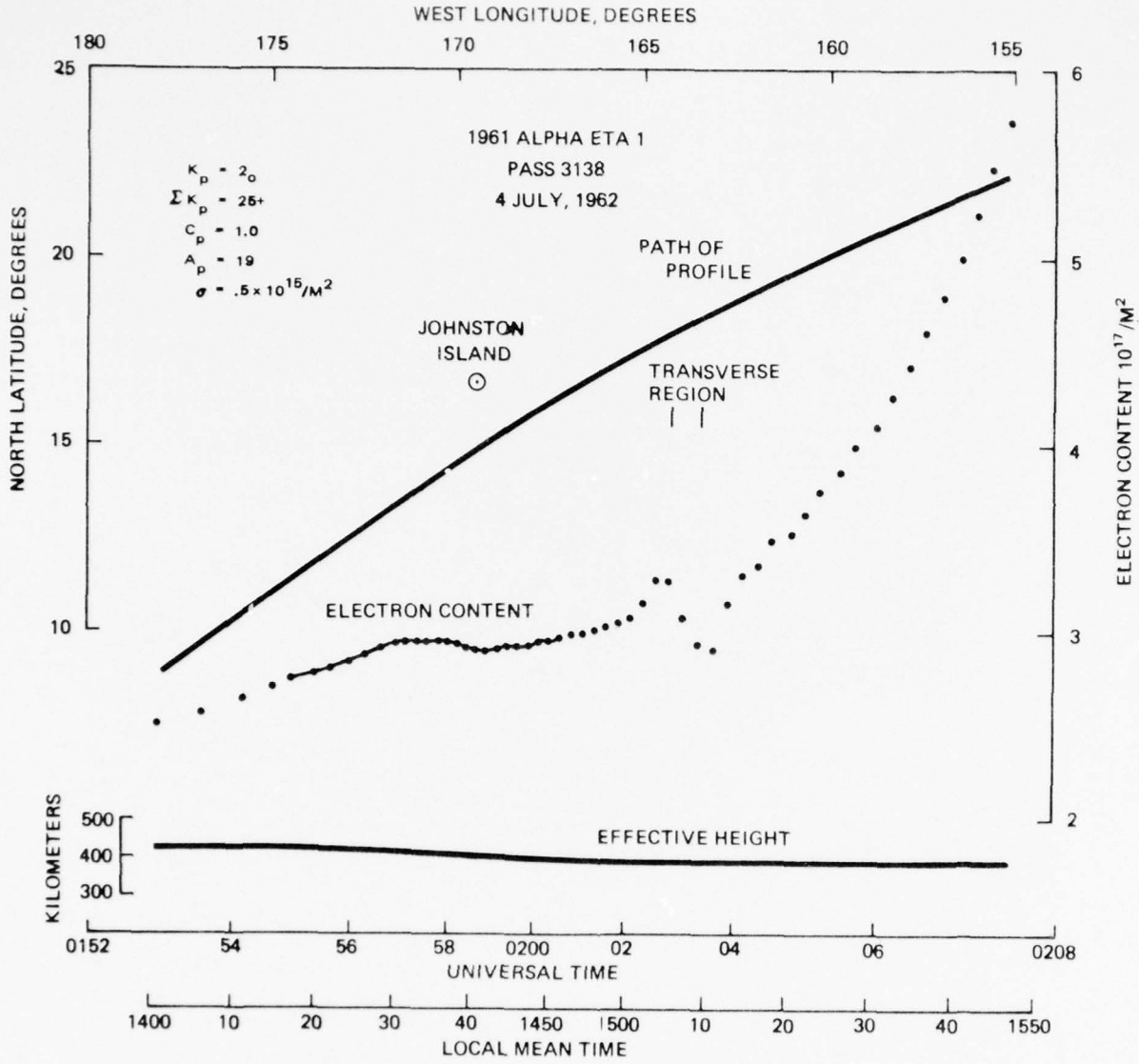

Figure 3.1 IONOSPHERIC ELECTRON CONTENT SHOWING STRONG HORIZONTAL GRADIENT

the aurorally disturbed ionosphere, HF signal absorption is very significant. In a series of experiments during the polar cap absorption (PCA) event in November 1969, the BRL measured HF and VHF absorption at intervals during the event. One such record is shown in Figure 3.2. Because collision frequency is strongly dependent on altitude, observed absorption is very sensitive to the altitude distribution of free electrons as well as the frequency employed. Further, because of the earth's magnetic field, the amount of absorption depends on the polarization of the transmitted signals.

C. Signal Refraction

As mentioned above, signal refraction, or bending, becomes marked when signal frequencies approach the plasma frequency of the medium. Under circumstances usually encountered in propagation problems, refraction occurs with little loss in signal energy (i.e., collision frequencies are much smaller than the signal frequency). Ionization gradients determine the radius of curvature of the refracted signal. Refraction is of great importance at HF and lower frequencies since it provides the mechanism for long-distance point-to-point communication for earth terminals. Refraction is of importance, also, for radio systems employing frequencies greater than HF for which line-of-sight bearing is very important. Target tracking radars fall into this important class of systems. Signal refraction, albeit small, produces significant target position errors. A technique, analogous to the dispersive doppler technique discussed in Section II, has been used to correct line-of-sight errors in target tracking systems. Two frequencies, with sufficient frequency separation, are used in the line-of-sight measurement. Measured angle differences in the lines-of-sight, together with an approximate model of the refracting medium, provide a method for estimating with good accuracy the true bearing, or line-of-sight, of a target being tracked. As in the trajectory comparison method described in Section II, the use of the affected system to determine self-inflicted ionospheric effects is a useful and effective method for a pragmatic determination and subsequent correction of errors caused by such effects.

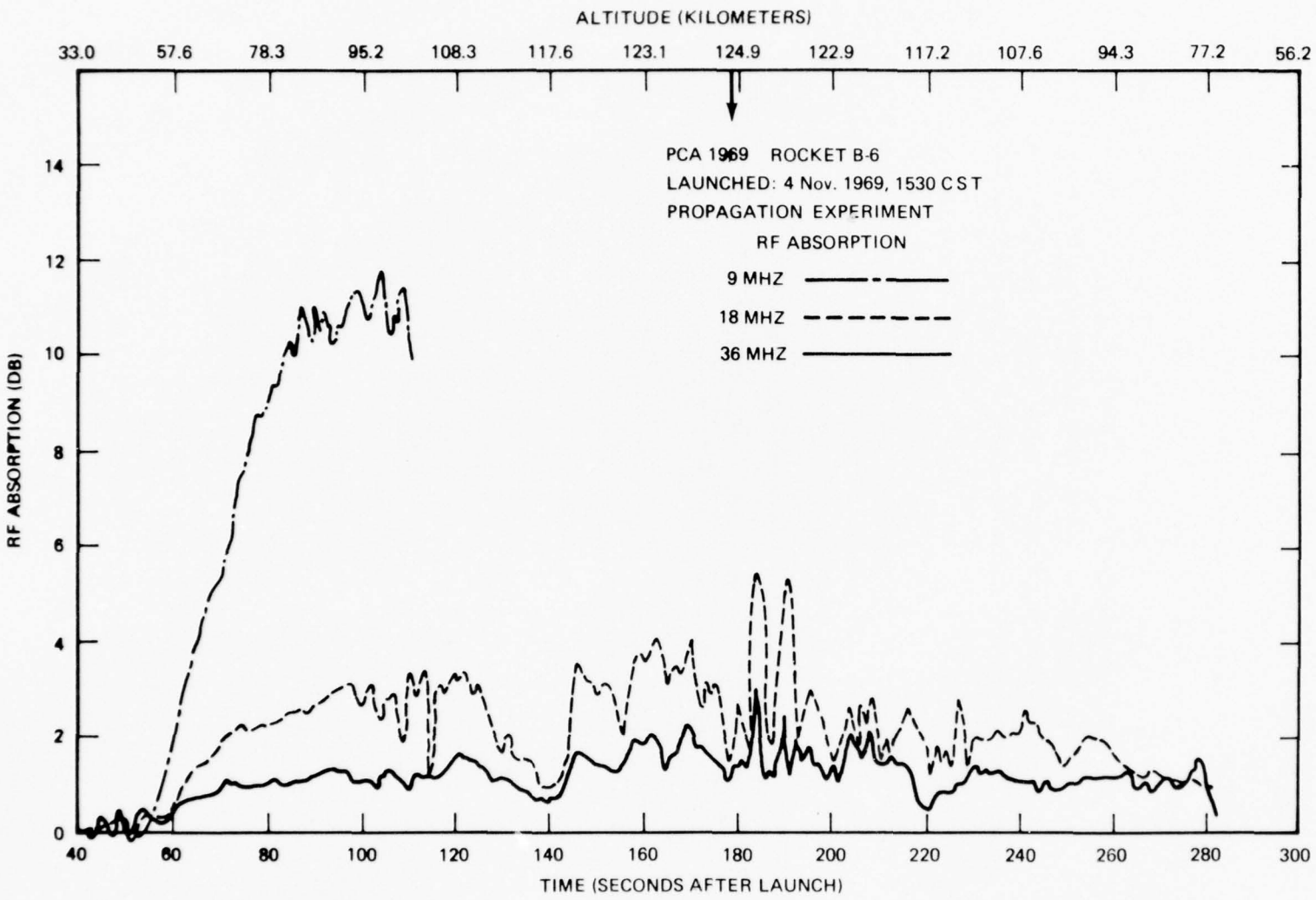

Figure 3.2 RF ABSORPTION FOR ROCKET B--6

D. Focusing, Defocusing, Multipath and Diffraction

Propagation problems falling under this general classification produce difficulties in all frequency regimes. Ionospheric discontinuities or significant gradients of size comparable to a few wavelengths of the transmitted signals produce large amplitude and phase fluctuations in received signals. Larger discontinuities can produce significant, but slower varying amplitude changes; because accompanying phase changes are also slow, effects on phase sensitive systems are not marked unless system margins are small (the order of a few db).

Ionospheric perturbations caused by rapidly varying particle precipitation (auroral regions and nuclear explosions), plasma-producing chemical releases such as barium, and nuclear-generated plasmas give rise to the propagation problems discussed in this section. In addition to measurements of ionospheric perturbations caused by high-altitude nuclear explosions, the BRL has carried out numerous propagation studies in the auroral regions and associated with barium releases.[10 23 24] For the latter, there are many and clear examples of the propagation effects relevant to the problems here discussed. Some, but not all, of the relevant BRL experiments are listed in Tables 1.2 and 1.3.

The discussion here will be limited to illustration of the propagation problems associated with ionized barium clouds. In Section IV, an illustration of auroral disturbance will be discussed. In Figure 3.3 is shown, schematically, the effect of a plasma "ball" (approximating a barium ion cloud) on radio signals transmitted in close proximity. The region indicated as "multipath" is also a region of focusing and diffraction. In October 1967, the BRL participated in an Air Force-sponsored chemical release program, HAVEN BARTER. The BRL experiment consisted of a three-frequency phase-coherent transmitter carried on the same vehicle from which the chemicals (barium) were released. The transmitter was "viewed" by two ground stations such that signals transmitted through and around the several barium ion clouds were observed. Figure 3.4 is a record of the 72 MHz

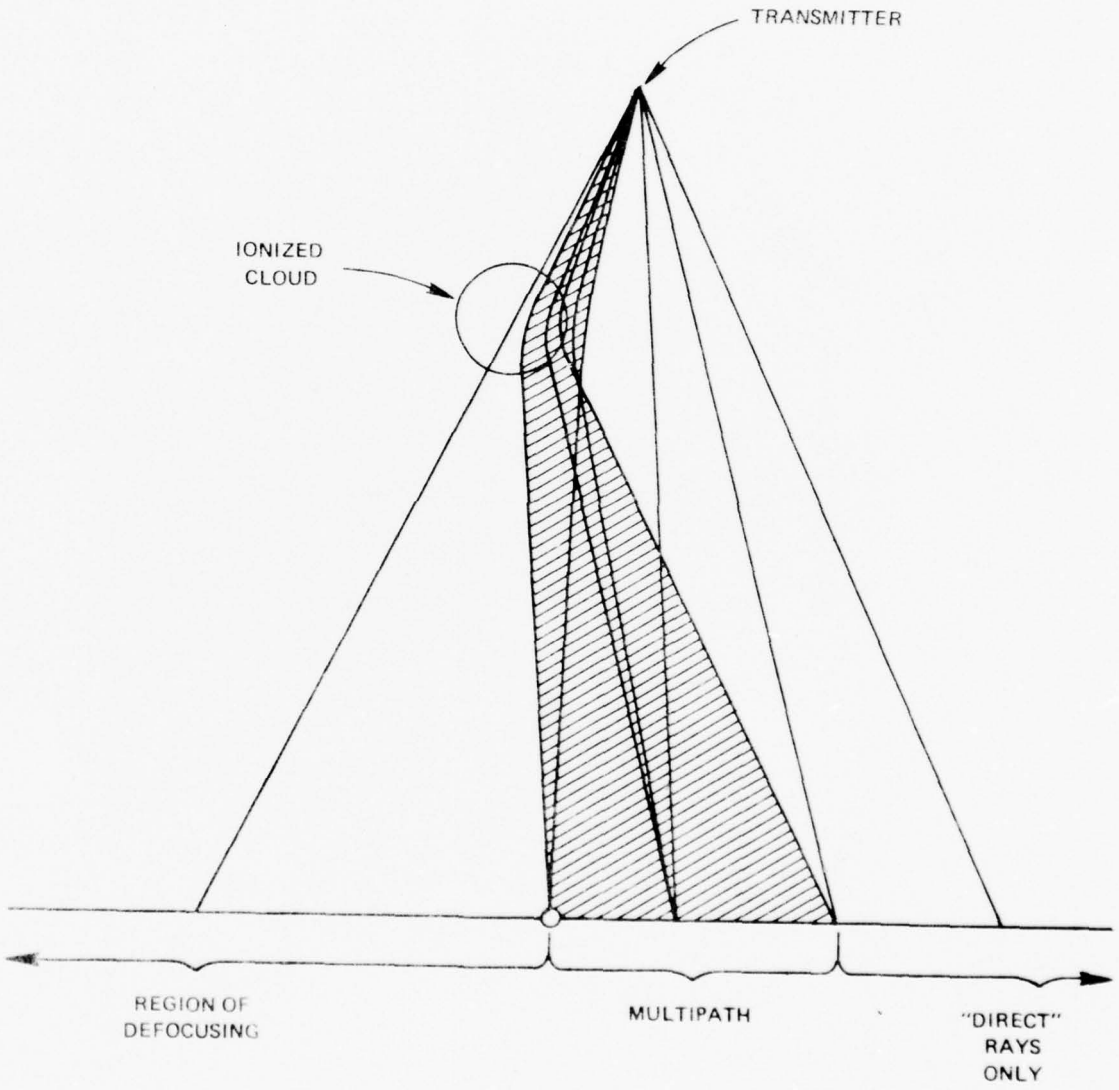

Figure 3.3 SKETCH ILLUSTRATING THE EFFECT OF AN IONIZED CLOUD ON PROPAGATION PATHS

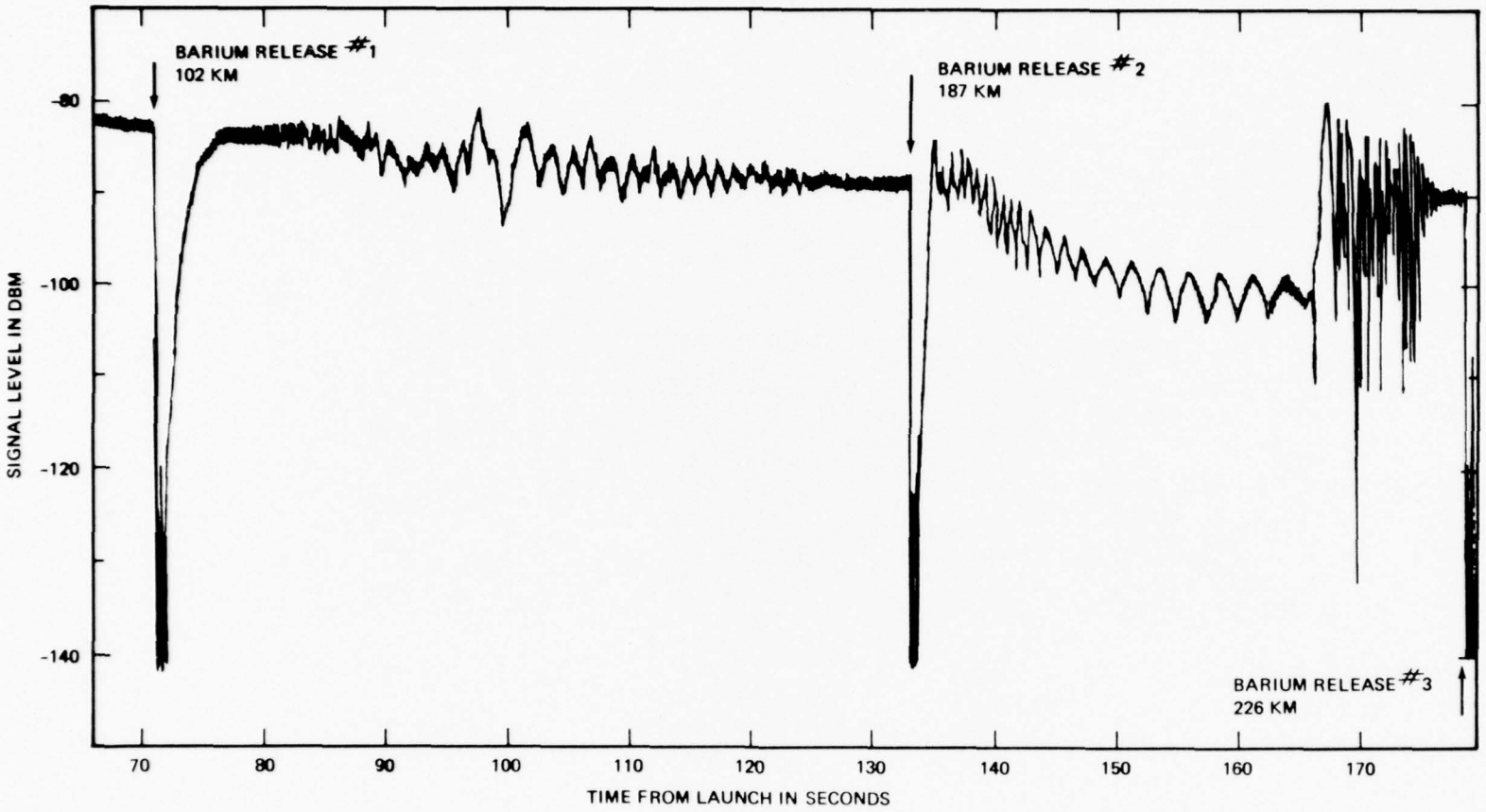

Figure 3.4 SIGNAL LEVEL OF 72MHz TRANSMISSION RECEIVED AT WALLOPS ISLAND LAUNCH SITE. PROJECT HAVEN BARTER

signal received by the ground station covered by the "footprint" of the ion clouds.[23] The several problems of propagation discussed in this subsection are clearly illustrated.

For each release, (Figure 3.4), thermal ionization in the exploding thermite charge caused immediate signal loss followed by signal recovery as the explosion products cooled and expanded. The first release was at such a low altitude that the barium cloud was confined to a small volume and the "footprint" of the cloud rather quickly moved away from the ground receiver due to rocket motion. Photoionization of the barium atoms has a time constant of approximately 15 seconds and the record shows the onset of multipath for signals reaching the receiver at approximately 15 seconds after the release and continuing for approximately 30 seconds, by which time the receiver viewed the direct rays only. The second release expanded to a substantially larger volume and the "footprint" for that release covered the ground receiver for approximately 35 seconds. The record from 135-165 seconds illustrates *multipath* (higher frequency oscillations) and the signal attenuation arising from defocusing by the plasma "ball". The increase in attenuation with increasing time simply reflects the photoionization time constant for barium atoms. Shortly after 165 seconds, the rocket transmitter "comes out from behind" the ion cloud and the receiver observes strong scintillation arising from diffraction and multipath effects. At the same time, the phase-lock tracking loops employed in the receivers lost lock indicating phase changes too rapid for the receivers to follow. As a rough approximation, phase rates-of-change of at least 700 radians per second were encountered.

Experiments similar to the HAVEN BARTER experiment just described were conducted during the SECEDE II project in the winter of 1971 (see Table 1.3). For these experiments, a multi-frequency transmitter was carried by a separate rocket, and occultations by the barium ion clouds occurred substantially later than the HAVEN BARTER occultations. Again similar effects were observed with severe phase and amplitude scintillation just prior to and after occultation. For the SECEDE II releases, four receiving stations were operated and it was possible, because of spatial separations, to model the

ion cloud as seen at radio frequencies. The model was constructed by assuming an ellipsoidal ion cloud distribution with self-consistent cross sections as observed from the four receiving ground stations.[24] The geometrical and ionization parameters of the ellipsoid were then adjusted to match the dispersive phase measurements for each of the stations. The results of this modeling procedure are shown in Figures 3.5 and 3.6. The BRL experiments in SECEDE II illustrate a powerful method of determining the effects of localized plasma concentration and distribution on radio signal transmissions. The process of constructing a radiofrequency model provides a credible mechanism for predicting effects of such distributions for other frequency regimes.

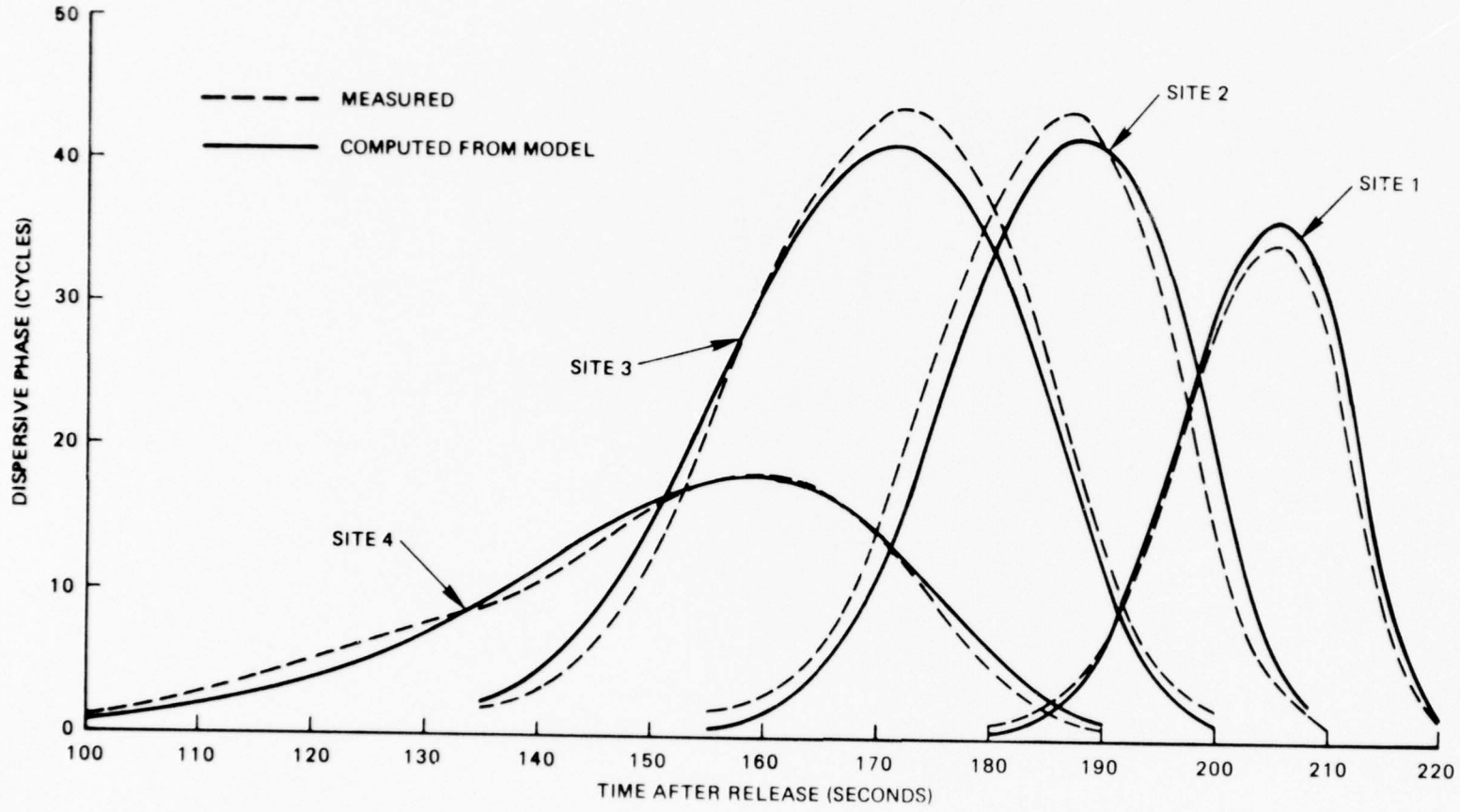

Figure 3.5 291/874 MHz DISPERSIVE PHASE VERSUS TIME FOR THE PLUM CLOUD.

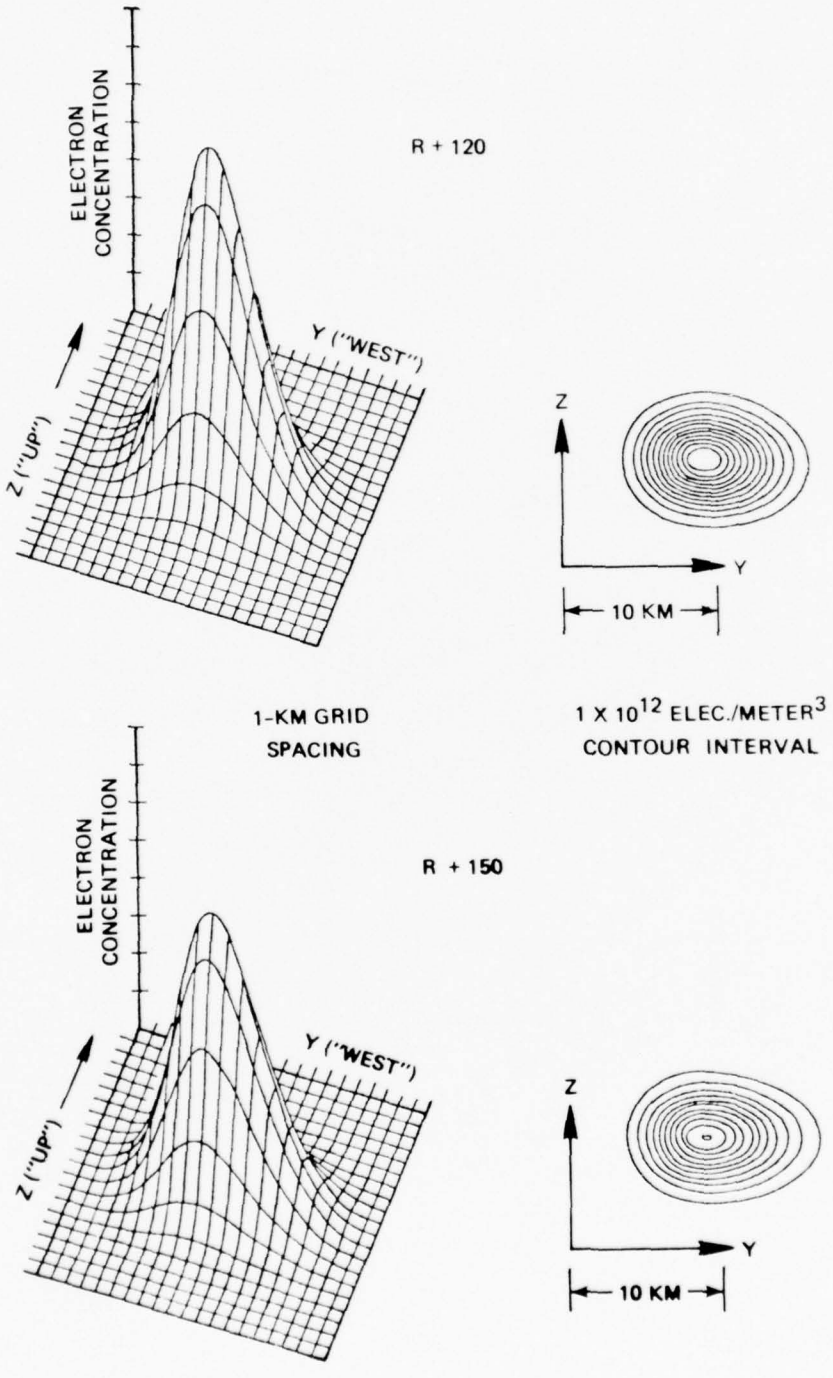

Figure 3.6 ELECTRON CONCENTRATION IN A SLICE THROUGH THE PLUM CLOUD MODEL, PERPENDICULAR TO THE MAGNETIC FIELD, AT 120 AND 150 SECONDS AFTER RELEASE

IV EXAMPLE SELECTED FOR ANALYSIS

In the previous section the several kinds of propagation problems giving rise to communications degradation were discussed. Each of the problems can be illustrated in the propagation experiments conducted by the BRL; the nature of the experiments provided data to permit a quantitative estimate of effects on communications systems at radiofrequencies employed during the experiments and at other frequencies as well. In this section, one propagation problem is analyzed using results from the BRL experiments. A second problem quite appropriate for analysis with the BRL data is that of collision frequencies in the lower D-region. Collision frequencies are in themselves not a problem but their proper value can become quite important for estimation of signal absorption in the presence of high electron densities in the lower D-region. Such high densities did occur in the polar cap absorption (PCA) event in November 1969[11] (and see Figure 4.4). Using signal absorption measured during the event,[25] it was possible to compare calculated and measured differential absorption, but the comparison was carried out for just one frequency at one time and with an assumed electron-neutral collision frequency.[26] Other work[27] suggests that collision frequencies could vary by a factor of three in the lower D-region; in the presence of high electron densities, this variation can markedly alter signal absorption. A considerable number of absorption measurements were made by the BRL during PCA 69 and these data probably warrant further analysis in the context of looking for collision frequency variability (if such exists) and for the best numerical values corresponding to conditions during PCA 69.*

Focusing and Defocusing of Signals

In the natural ionosphere, the focusing and defocusing of radio signals result from propagation through plasma "holes" or "blobs", respectively. The magnitude of the effect depends primarily on ionization gradients normal to the direction of propagation. In the natural ionosphere, the strongest

* Since the preparation of this brief report, attention has been called to a recent report by W. Swider and I.L. Chidsey in which the radiofrequency absorption data were analyzed in context of the further study suggested here. ("Calculated and Measured HF/VHF Absorption for the 2-5 November 1969 Solar Proton Event," Air Force Geophysics Laboratory TR-76-0053, March 1976.)

gradients most likely occur in the auroral region where strong variations, in time and place, occur in the deposition of ionizing particles. During the PCA 69 experiments at Ft. Churchill, Canada, signal focusing and defocusing was encountered on two occasions. Data from the propagation experiment are analyzed in this section to provide a semiquantitative picture of postulated plasma blobs in the auroral ionosphere. Such a picture is useful only to indicate the ionization gradients possible and the size of the ionization inhomogeneities. The picture does provide a model for estimating effects on communications systems operating at frequencies other than those used in the BRL experiments and for geometries for which transmission through a number of blobs may occur.

As indicated earlier, a ray-trace analysis is required for accurate representation of signal attenuation under conditions of defocusing by a complex plasma blob. Such an analysis is beyond the scope of this report in the context of deriving a semiaccurate picture of the ionization inhomogeneities encountered in PCA 69. Rather, an approximate analysis method is used which does provide a useful insight into the conditions encountered. This simple analysis provides answers in good agreement with measured attenuations for the HAVEN BARTER barium release and for which a ray-trace analysis was carried out.

In the HAVEN BARTER experiment, the combined dispersive doppler and attenuation measurements gave the following derived parameters for the barium plasma cloud (gaussian distribution of Ba ions assumed):[23]

Time constant, τ, = 15 sec.

Limiting Total Cloud Inventory, $TI_{LIM} = 7.0 \times 10^{23}$ ions (or electrons)

Scale Radius squared, $h_G^2 = 4.3 + 0.031(t)$, km^2

and

$N = N_o \exp\left(-r^2/h_G^2\right)$, electron distribution in cloud as function of radius

$h_G^2 = (h_{G_o}^2) + 4Dt$

$TI = TI_{LIM} (1-\exp^{-t}/\tau)$ = ion inventory as function of time

N_o = peak electron density at center of cloud

t = time after release of the barium cloud

D = ion diffusion coefficient (approximately $7.5 \times 10^{-3} km^2 sec^{-1}$ as derived from the experiment)

h_G = radius of cloud at which $N = N_o/e$

For the simplified analysis, the barium plasma was assumed to be a sphere of uniform density and radius h_G. The density is given by,

$$N' = TI \left\{(4/3)(\pi h_G^3)\right\}^{-1}$$

Using these simplifying assumptions and the schematic shown in Figure 4.1, an expression for signal attenuation in transmission through the spherical plasma can be derived. Referring to Figure 4.1, the following relationships hold:

$$\sin \alpha = L(\sin \theta)/R \tag{4.1}$$

$$\sin \beta = \sin \alpha \, \mu^{-1} \quad \text{(Snell's Law)} \tag{4.2}$$

μ = index of refraction $\doteq [1-(80.5 N')/f^2]^{1/2}$

N' = electron density (m^{-3})

f = transmission frequency (hz)

$$\sin \beta = \sin \alpha \, [1-(80.5N/f^2)]^{-1/2} \tag{4.2}$$

$$\xi = \alpha - \theta \tag{4.3}$$

$$\gamma = 180-2\beta \tag{4.4}$$

$$\theta' = 180-\alpha-(\gamma+\xi) = \theta+2(\beta-\alpha) \tag{4.5}$$

$$\Delta H = R \sin \alpha / \sin \theta' \tag{4.6}$$

Attenuation of the radio signal transiting the spherical plasma is calculated by noting that the signal power radiated in the small solid angle, represented by θ, is spread by refraction into a solid angle represented by θ'. Reduction in signal power by such refraction is, simply,

$$P_2/P_1 \equiv A_1/A_2$$

$$P_2/P_1 = \left\{(L+H)^2\tan^2\theta\right\}\left\{(H+\Delta H)^2\tan^2\theta'\right\}^{-1} \qquad (4.7)$$

where A_1 and A_2 are areas on the ground illuminated by energy contained in the solid angles represented by θ and θ'; P_1 and P_2 are the received power per unit area in the absence and presence of the spherical plasma, respectively. The signal attenuation, then, is given by,

$$\text{Attenuation (db)} = 10 \log \left\{(L+H)^2\tan^2\theta\right\}\left\{(H+\Delta H)^2\tan^2\theta'\right\}^{-1} \qquad (4.8)$$

The result predicted by Equation 4.8 may be seriously questioned in light of the radical assumption of uniform electron density distribution in a refracting sphere rather than a quasi-gaussian distribution in a plasma more closely resembling a prolate spheroid. Some compensation does occur in that the radius of the real plasma is somewhat greater than the radius assumed so that total refraction of the transiting radio signal is approximately the same for the real and assumed plasma distribution. Further, the peak electron density, $N_o \approx 9 \times 10^{12} m^{-3}$, derived from the ray-trace model is reasonably close to the $N' = 1.3 \times 10^{13} m^{-3}$ used in the approximation.

The attenuation predicted by Equation 4.8 is compared to measured data and the ray-trace analysis in Table 4.1. Measured data, comparable to those shown in Figure 3.4, are available for the 36 and 146 MHz transmissions.[23] The comparison for 146 MHz is not valid in that measured attenuation was effectively zero at times corresponding to maximum attenuation at 36 and 73 MHz. The maximum measured attenuation at 146 MHz occurred at approximately 10 seconds after plasma release at which time measured attenuations at 36 and 73 MHz were approximately half their maximum value. In effect, the "footprint" of the plasma cloud for the 146 MHz transmission did not cover the receiving station at 30 seconds after plasma release.

An examination of attenuation predicted by Equation 4.8, and with reference to Figure 4.1, shows that the most sensitive parameter, by far, is the

Table 4.1

MEASURED vs PREDICTED MAXIMUM ATTENUATION, HAVEN BARTER RELEASE NO. 2
(Approximately 30 Seconds After Release)

	Frequency[1]		
	36 MHz	73 MHz	146 MHz
Measured	-30^{+5}_{-10} db	-12 ± 2 db	-2.5 ± 1 db[2]
Ray-Trace Analysis	-28 ± 1.2 db	-8.3 ± 0.6 db	--
Predicted by Equation 4.8	-33 db	-12 db	-5 db

[1] Rounded to nearest MHz.

[2] Measured at approximately 10 seconds after release.

plasma electron density. For the realistic case in which a uniform electron density is replaced by a plasma with density gradients, the ionization gradient becomes an important parameter. Removing the transmitter to greater distances from the plasma cloud (parameter L in Figure 4.1) is effective in reducing the "footprint" of the cloud as seen from the ground. The effect of increased L in Equation 4.8 is compensated by a decrease in θ so that attenuation within the footprint remains approximately the same.

Attenuation data representing plasma defocusing for HAVEN BARTER, SECEDE III and PCA 69 are shown in Figure 4.2.[23 11 10] The attenuation values shown for HAVEN BARTER and the GUM and ELM-2 releases in SECEDE III are reasonably consistent in that larger barium payloads were used in the SECEDE experiments. The attenuation for ELM-1 appears inconsistent in that the barium ion yields for ELM-1 and ELM-2 were very similar. The most likely explanation for the marked differences in the ELM releases derives from the different release altitudes. ELM-1 was released at 140 km and confinement of the release by the ambient atmosphere was substantially greater than for the higher release. Even so, the maximum electron density indicated for ELM-1 was close to 10^8 m^{-3}, a value perhaps three times greater than peak densities (mostly inferred) in other barium releases.

For a natural disturbance in the auroral regions, such as that produced by a polar cap absorption (PCA) event, the simple picture of a "plasma ball" giving rise to abnormal attenuation is scarcely adequate. Figure 4.3[11] shows measured attenuation during flight of an early rocket (B-2) in the PCA event of November 1969. The absence of appreciable attenuation before 125 seconds of flight indicates a relatively low concentration of electrons below 80 kilometers. Electron densities derived from dispersive phase measurements are shown in Figure 4.4 and substantiate the low attenuation (absorption in this case) measured on flight B-2. Beginning at approximately 125 seconds (t_1) a marked enhancement (focusing) of the signal occurs followed at 140 seconds (t_2) by the onset of strong attenuation (defocusing) of the signal. The period of abnormal attenuation may be interpreted as rocket overflight of a small region of enhanced electron density arising from particle deposition below the rocket. A highly schematic representation

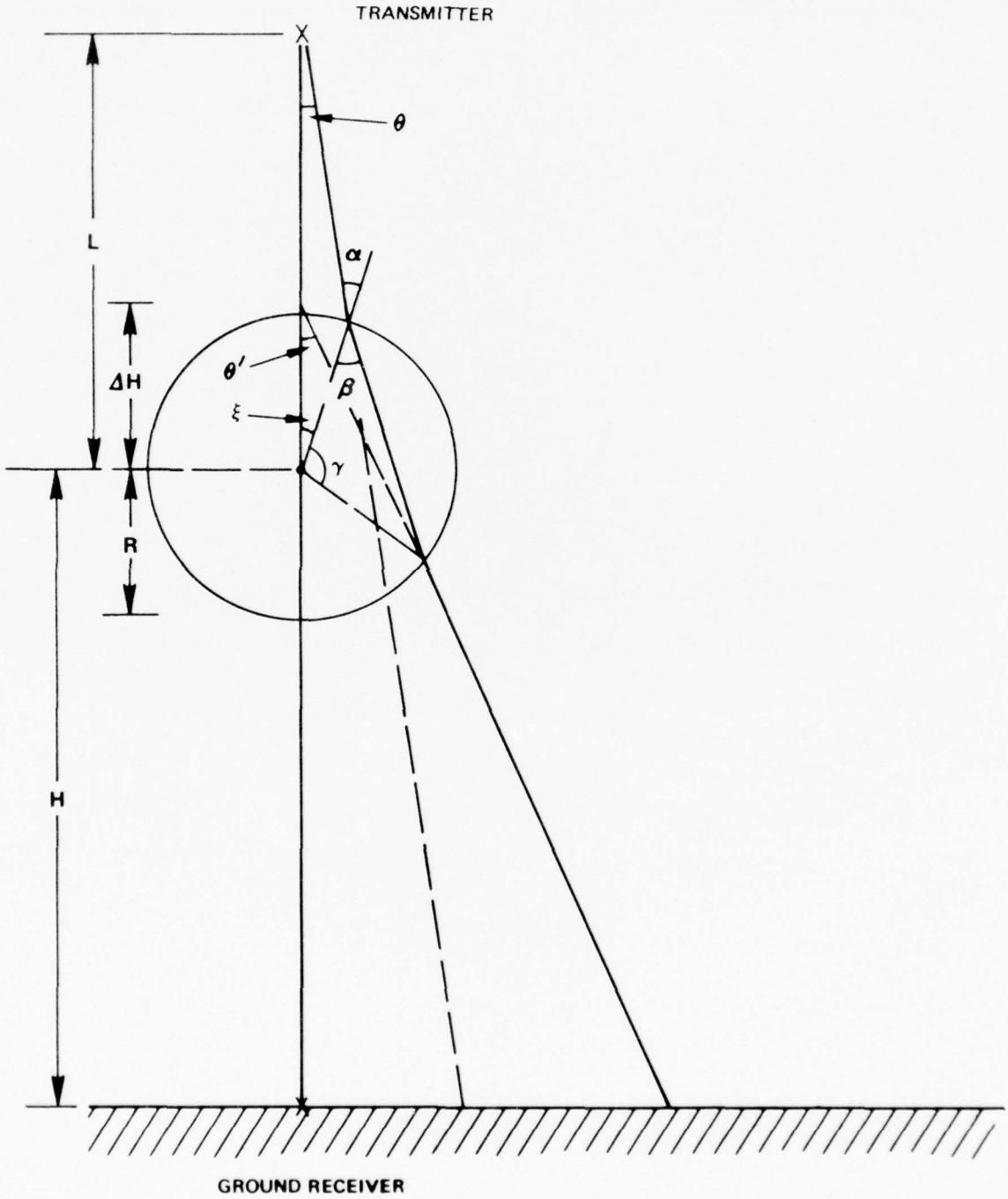

Figure 4.1 PLASMA SPHERE REFRACTION

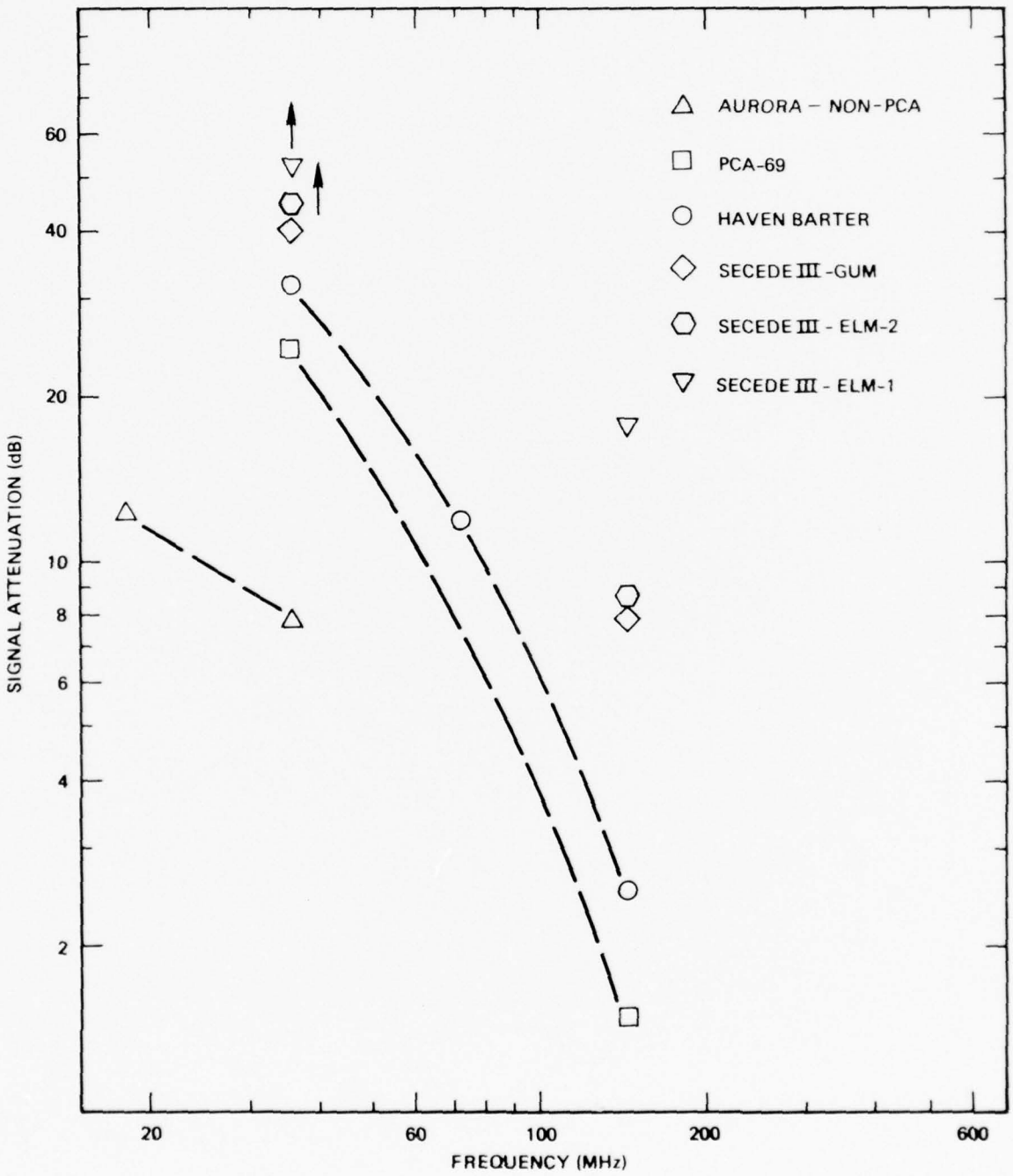

Figure 4.2 ATTENUATION FROM SIGNAL DEFOCUSING

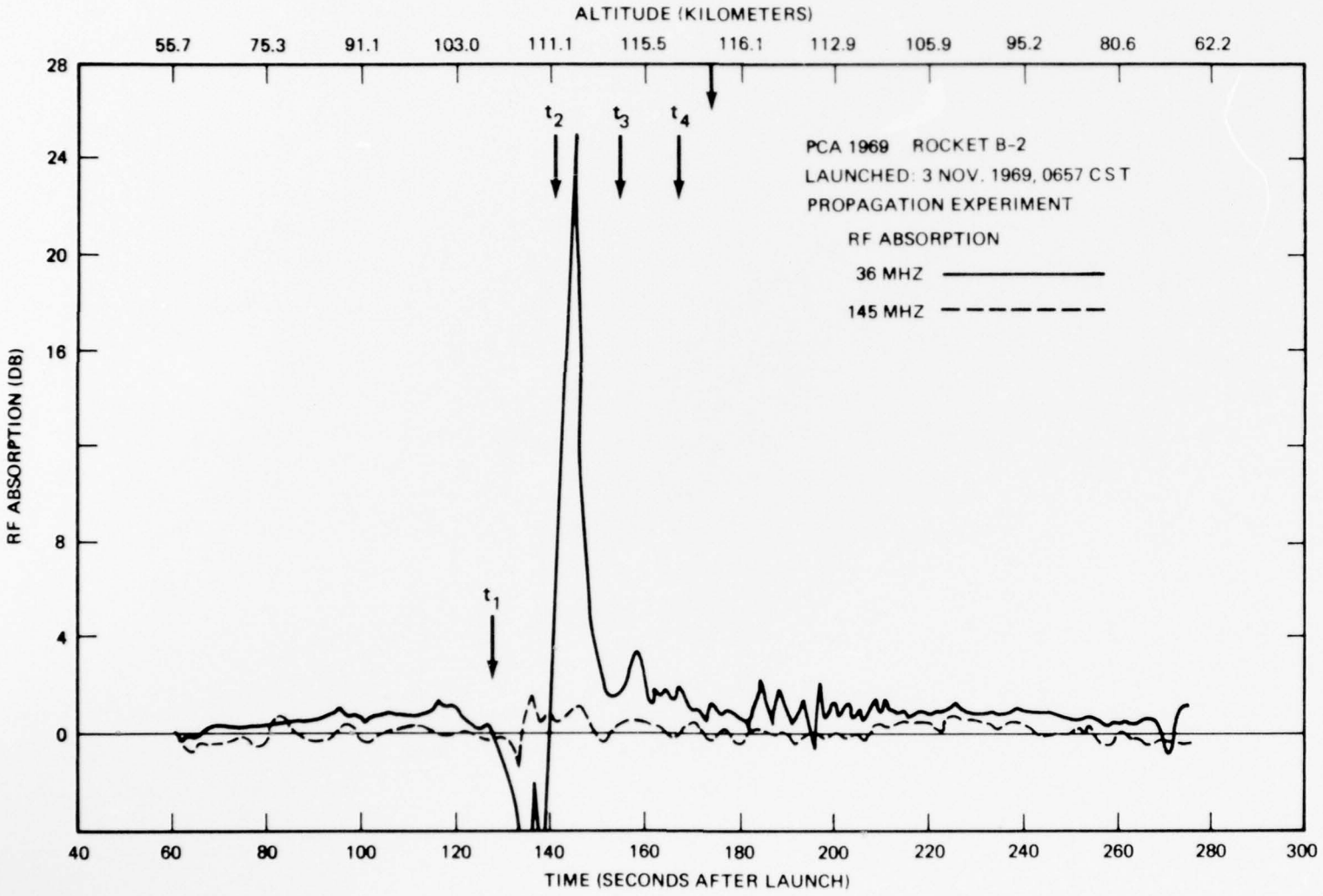

Figure 4.3 RADIO FREQUENCY ATTENUATION ILLUSTRATING FOCUS/DEFOCUS

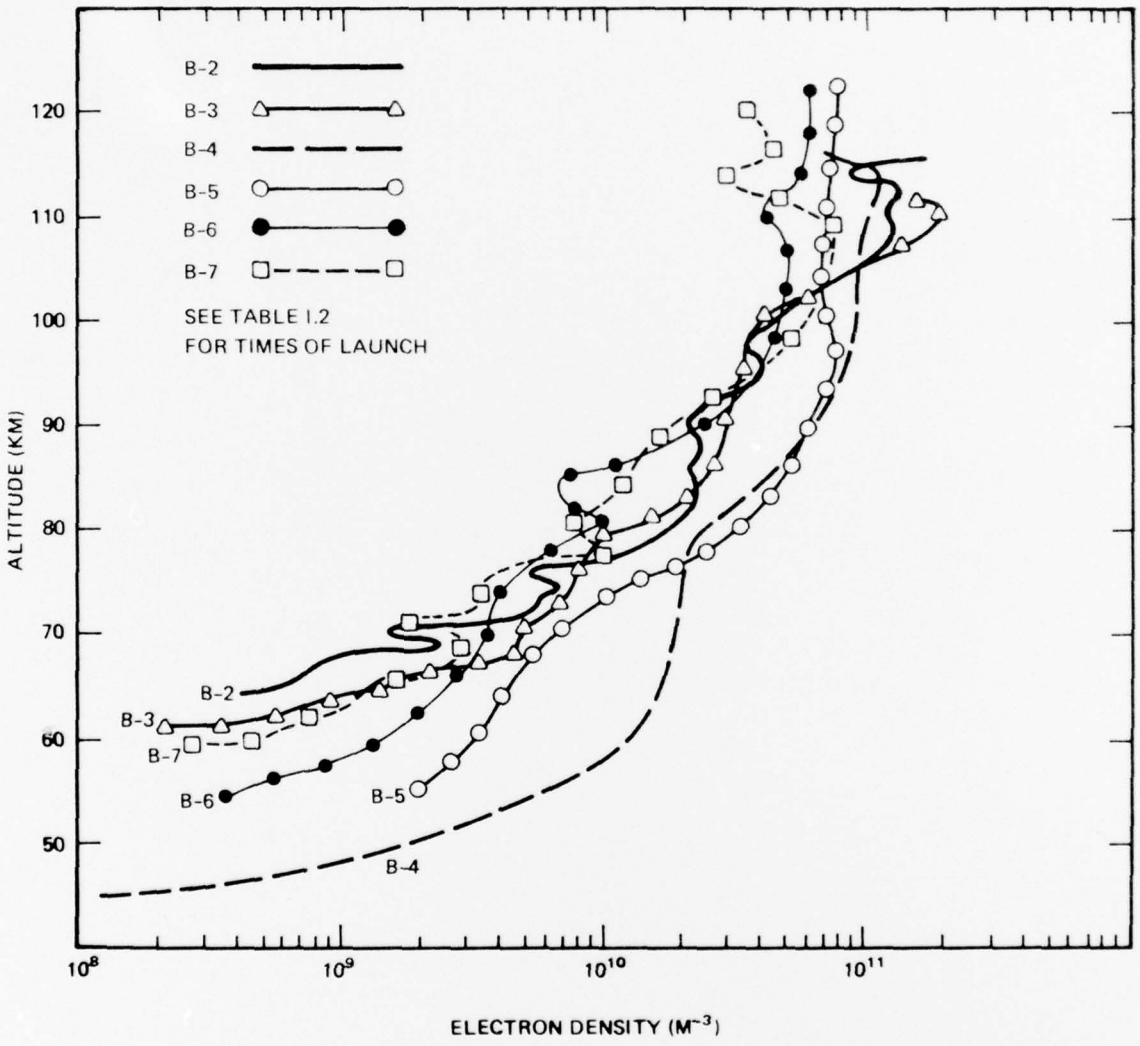

Figure 4.4 PCA–69 ELECTRON DENSITY PROFILES

of the disturbance cross section (in the trajectory plane) is shown in Figures 4.5 and 4.6. The times t_1, t_2, etc., shown in Figures 4.3 and 4.6 roughly correspond. The height of the disturbance, h_D, is constrained in that it must be below the rocket but above the region (above 80 km) of large absorption; the size is constrained by the short duration of the large signal attenuation. If, for example, the discontinuity ("blob") were at an altitude of 90 km, the horizontal motion of a raypath at that altitude is approximately 2.5 km between 120 and 160 seconds of flight time. There is a major constraint, also, on the electron density in the discontinuity in view of the data shown in Figure 4.4. These several constraints make it possible to estimate the size and character of the discontinuity despite the highly fictitious representation shown in Figure 4.1 and the attenuation expression derived therefrom.

From Equation 4.8, the ratio $(\tan^2\theta)/(\tan^2\theta')$ clearly dominates in determining the attenuation. From Equations 4.1, 4.2, 4.5, 4.8 and the measured attenuation of -26 db (Figure 4.3) for 36 MHz, a "blob" density of $3\text{-}5\text{x}10^{11}$ electrons m^{-3} and a "blob" diameter of 200 meters at 10-15 kilometers below the rocket provides an approximate fit to the data. The calculated attenuation for this representation of the discontinuity is extremely sensitive to electron densities assumed and the size of the discontinuity. Larger electron densities are essentially prohibited by the very high ionization rates required; a density of $3\text{x}10^{11}$ requires highly localized ionization rates of the order of 10^{10} ion pairs m^{-3} sec^{-1}, a value approximately 5 times greater than measured by other experiments during the PCA 69 event.[12] At altitudes below 90 km, the increasing recombination rates would require still higher ionization rates for a given electron density.[29]

The thrust of the above analytical argument and representation of the ionization discontinuity is not that the measured attenuations can provide a picture of the ionization structure during the highly disturbed conditions encountered in the auroral regions but rather that there is a physical basis for the observations. From the standpoint of communication the existence of blobby structures provides a mechanism for signal loss in

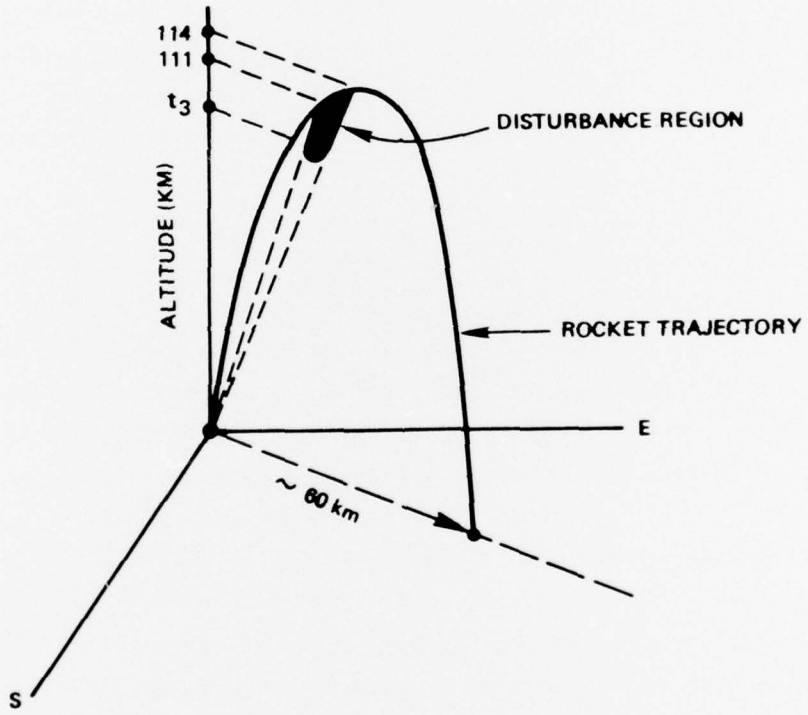

Figure 4.5 FLIGHT SCHEMATIC, ROCKET B–2

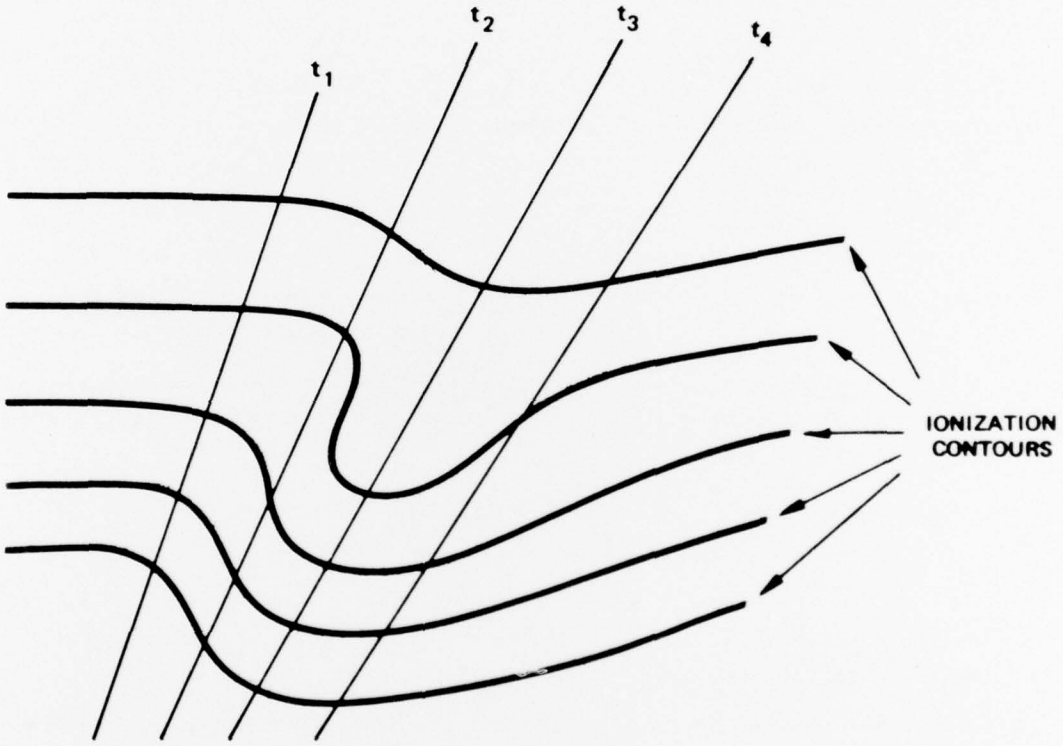

Figure 4.6 RAY PATHS THROUGH POSTULATED DISTURBANCE

addition to the more commonly observed absorption of signal energy arising from relatively high ionization at lower altitudes and attendent electron-neutral collisions. Considering the fact that anomalous attenuation was observed on two rocket flights at Ft. Churchill and probably occurred on one of the flights during the 1969 SECEDE III experiments at Poker Flat, Alaska,[10] the occurrence of signal defocusing in auroral regions would appear statistically significant.

The presence of sharp discontinuities in ionization gives rise to another potential problem for phase coherent communications systems. For the HAVEN BARTER plasma releases, the phase-lock loop operating at 36 MHz could not track at the time the radio signals passed the edge of the barium ion cloud (approximately 170 seconds in Figure 3.4). This loss of phase coherence arises mainly from multipath for signals grazing the region of high ionization. A similar situation arose during flight of the B-2 rocket in the PCA 69 experiments. For this flight, dispersive phase was obtained from the coherent pairs of frequencies, 36/145 MHz and 145/583 MHz. Starting at approximately 130 seconds (see Figure 4.3), phase lock was lost for the 36 MHz signal, most likely from severe multipath, with an accumulated phase loss of approximately 30 radians which was never recovered.

Certainly the most spectacular example of a highly disturbed natural ionosphere during any period of observations by the BRL group occurred during the IGY. At that time, ionospheric effects were determined by the relatively crude trajectory comparison method and Faraday rotation of the two-way DOVAP signals. The DOVAP system was tracking an Aerobee-Hi rocket launched at 0025 CST from Ft. Churchill on 24 November 1958. The vehicle flew into a weak aurora but the effect on the tracking system was dramatic. Rapid phase shifts and fading of the 37 MHz signals degraded tracking accuracies to the extent that the trajectory comparison method could not be used. Faraday rotation data indicated onset and overflight of regions of extremely enhanced electron density (both up-leg and down-leg) with very sharp density gradients. An estimate of 2×10^{13} electrons m^{-3} in a very small volume, and at an altitude less than 120 km, gives some match to the observed data.[18]

Knowledge of the existence and some quantitative measure of attenuation and multipath associated with blobby plasma structures in the natural ionosphere makes possible compensations in communications systems operating in that environment. Much more difficult and potentially serious are these same effects on signal strength and signal phase in the severe environment produced by high altitude nuclear events.

V SUMMARY AND CONCLUSIONS

Previous sections have given a most cursory review of efforts at the Ballistic Research Laboratories in their studies of radio propagation through the ionosphere. Following rocket experiments in Kauai in 1971, personnel and work reassignments together with a disappearing mission led to termination of upper atmosphere research with rocket sounding techniques. A vigorous laboratory program for studying atmospheric chemistry reactions relevant to altitudes of interest to the BMD program was continued and complex balloon-borne experiments were initiated. However, a capability for atmospheric research with rockets by the BRL is probably beyond recall.

There have been many contributions by the BRL in propagation research not touched upon or referenced in this report. Work in antenna theory and design together with the development of equipments for the reception and processing of extremely weak signals was found in the vanguard of these technologies. The development of digital ray tracing techniques was an important contribution. The use of dispersive doppler information from spaced ground receivers to describe plasma structure was an unusual application of the BRL propagation studies.

In the long run, BRL measurements of propagation effects in the auroral and nuclear disturbed ionospheres will constitute an important if not major part of the available data base for such disturbances. Nuclear tests in the atmosphere are not foreseeable in the near future, and there is no assurance that natural disturbances of the magnitude seen in IGY will be available against which to test communications systems of the future.

BIBLIOGRAPHY

[1] Berning, W.W., "Determination of Ionospheric Charge Densities from DOVAP Records," Ballistic Research Laboratories Report No. 745, 1950.

[2] Khore, A.J., D.L. Cain, et al., "Occultation Experiment: Results of the First Direct Measurements of Mars' Atmosphere and Ionosphere," Science, 149, 1243, 1965.

[3] Fjeldbo, G., and V.R. Eshleman, "The Atmosphere of Mars Analyzed by Integral Inversion of the Mariner 4 Occultation Data," Planetary and Space Science, 16, 1035, 1968.

[4] Howard, H.T., G.L. Tyler, et al., "Venus: Mass, Gravity Field, Atmosphere, and Ionosphere as Measured by the Mariner 10 Dual-Frequency Radio System," Science, 183, 1297, 1974.

[5] Whitten, R.C. and L. Colin, "The Ionospheres of Mars and Venus," Reviews of Geophysics and Space Physics, 12, 155, 1974.

[6] Seddon, J.C., "Propagation Measurements in the Ionosphere with the Aid of Rockets," Jour. Geophysical Research, 58, 323, 1953.

[7] Marks, S.T., C.E. Shafer, W.J. Cruickshank, R.E. Prenatt, and G.A. Dulk, "Summary Report on Strongarm Rocket Measurements of Electron Density to an Altitude of 1500 Kilometers," Ballistic Research Laboratories Report No. 1187, 1963.

[8] Berning, W.W., Unpublished.

[9] Dean, W.A., "Ambient Electron Density Profiles-Project SECEDE II," Ballistic Research Laboratories Report No. 1825, 1975.

[10] Dean, W.A., "Auroral Zone Electron Density Profiles-Project SECEDE III Rockets," Ballistic Research Laboratories Memorandum Report No. 2078, 1970.

[11] Dean, W.A., and I.L. Chidsey, "Final Report on BRL Participation in Operation PCA 69," Ballistic Research Laboratories Report No. 1669, 1973.

[12] Ulwick, J.C. (Editor), "Proceedings of COSPAR Symposium on Solar Particle Event of November 1969," AFCRL Special Report 144, 1972.

[13] Zancanata, H.W., "Catalogue of Upper Atmospheric Research Probes (Gun and Rocket Launched) and Balloon-Borne Instrumentation Instrumented by the Ballistic Research Laboratories from 1956 through 1972." Ballistic

[14] Hammond, A.L., "Solar Variability: Is the Sun an Inconstant Star?," Research News, Science, 191, 1159, 1976.

[15] Chidsey, I.L., "Low Latitude Electron Content and Ionospheric Height from a Hybrid Faraday-Doppler Program," Ballistic Research Laboratories Report No. 1425, 1968.

[16] Dean, W.A., and H.T. Lootens, "Ionosphere Measurements with a Four-Frequency Phase Coherent Beacon," Ballistic Research Laboratories Report No. 1396, 1968.

[17] Dean, W.A., "Resolution of Ambiguities in Dispersive Doppler by Modulation Techniques," Ballistic Research Laboratories Report No. 1359, 1967.

[18] Prenatt, R.E., and J.C. Mester, "Measurement of Electron Density from IGY DOVAP Records," Ballistic Research Laboratories Report No. 1198, 1964.

[19] Davies, K., "Ionospheric Radio Propagation," National Bureau of Standards Monograph 80, 1965.

[20] deMendonca, F., and O.K. Garriott, "Ionospheric Electron Content Calculated by a Hybrid Faraday-Doppler Technique," Jour. Atmospheric and Terrestrial Physics, 24, 317, 1962.

[21] Dulk, G.A., "Faraday Rotation Near the Transverse Region of the Ionosphere," Jour. Geophysical Research, 68, 6391, 1963.

[22] Daniels, F.B., "Electromagnetic Propagation Studies with a Satellite Vehicle," Scientific Uses of Earth Satellites, University of Michigan Press, 1956.

[23] Prenatt, R.E., W.A. Dean, and W.W. Berning, "Electron Content of Barium Plasmas in the High Atmosphere," Ballistic Research Laboratories Report No. 1459, 1969.

[24] Prenatt, R.E., and G.A. Bowers, "The RF Transmission Experiment in SECEDE II and a Model for the Electron Concentration in the Ion Cloud from High Altitude Barium Release Plum," Ballistic Research Laboratories Report No. 1645, 1973.

[25] Chidsey, I.L., "Multifrequency Polar Cap Absorption Measurements, Proceedings of COSPAR Symposium on Solar Particle Event of November 1969," AFCRL Special Report 144, 307, 1972.

[26] Ulwick, J.C., "Comparison of Black Brant Rocket Measurements of Charged Particle Densities during Solar Particle Events," Ibid, 395.

[27] Belrose, J.S., and I.A. Bourne, "The Electron Distribution and Collision Frequency Height Profile for the Lower Part of the Ionosphere (The D and Lower E Regions)," Conference Proceedings, Ground-Based Radio Wave Propagation Studies of the Lower Ionosphere, Defence Research Board, Department of National Defence, Canada, 79, 1967.

[28] Lootens, H.T., and R.E. Prenatt, "Re-evaluation of Fish Bowl Project 6.3 Electron Density Profiles," Ballistic Research Laboratories Memorandum Report No. 1865, 1967.

[29] Sivider, W., and W. A. Dean, "Effective Electron Loss Coefficient of the Disturbed Daytime D Region," Journal of Geophysical Research, 80, 1815, 1975.

DISTRIBUTION LIST

DEPARTMENT OF DEFENSE

Director
Command Control Technical Center
ATTN: C-650
ATTN: C-312, R. Mason

Director
Defense Advanced Rsch. Proj. Agency
ATTN: Nuclear Monitoring Research
ATTN: Strategic Tech. Office

Defense Communication Engineer Center
ATTN: Code R410, James W. McLean
ATTN: Code R820, R. L. Crawford

Director
Defense Communications Agency
ATTN: W. Heidig
ATTN: NMCSTS, G. C. Jones
ATTN: Code 480
ATTN: Code 810, R. W. Rostron

Defense Documentation Center
12 cy ATTN: TC

Director
Defense Intelligence Agency
ATTN: DT-1B
ATTN: W. Wittig, DC-7D

Director
Defense Nuclear Agency
ATTN: DDST
ATTN: STVL
ATTN: STSI, Archives
3 cy ATTN: RAAE
3 cy ATTN: STTL, Tech. Library

Dir. of Defense Rsch. & Engineering
Department of Defense
ATTN: DD/S&SS, John B. Walsh

Commander
Field Command
Defense Nuclear Agency
ATTN: FCPR

Director
Interservice Nuclear Weapons School
ATTN: Document Control

Director
Joint Strat. Tgt. Planning Staff, JCS
ATTN: JLTW-2
ATTN: JPST, Captain G. D. Goetz

Chief
Livermore Division, Fld. Command DNA
ATTN: FCPRL

Director
National Security Agency
ATTN: Frank Leonard
ATTN: W14, Pat Clark

OJCS/J-3
ATTN: WWMCCS, Eval. Ofc., Mr. Toma

DEPARTMENT OF DEFENSE (Continued)

Director
Telecommunications & Comd. & Con. Sys.
ATTN: Asst. Dir. (Sys)
ATTN: Scientific Advisor

DEPARTMENT OF THE ARMY

Chief of Engineers
Department of the Army
ATTN: F. DePierson

Commander
U.S. Army Communications Cmd.
ATTN: George Lane

Commander/Director
Atmospheric Sciences Laboratory
5 cy ATTN: DRSSEL-BL-SY-S, F. E. Niles

Chief C-E Services Division
U.S. Army Communications Cmd.
ATTN: CC-OPS-CE

Commander
Harry Diamond Laboratories
ATTN: DRXDO-RB, Robert Williams
ATTN: DRXDO-TI, Mildred H. Weiner
ATTN: DRXDO-NP, Francis N. Wimenitz
ATTN: DRXDO-NP

Commander
TRASANA
ATTN: EAB
ATTN: TCC/F. Payan, Jr.

Commander
U.S. Army Electronics Command
ATTN: DRSEL-PL-ENV, Hans A. Bomke

Chief
U.S. Army Research Office
ATTN: A. Dodd

Commander
U.S. Army Foreign Science & Tech. Ctr.
ATTN: P. A. Crowley
ATTN: R. Jones

Commander
U.S. Army Materiel Dev. & Readiness Cmd.
ATTN: DRCDE-D, Lawrence Flynn
ATTN: DRCLDC, J. A. Bender

Commander
U.S. Army Missile Command
ATTN: DRSMI-YTT, W. G. Preussel, Jr.

Commander
U.S. Army Nuclear Agency
ATTN: ATCA-NAW, J. Berberet

Director
U.S. Army Ballistic Research Laboratories
10 cy ATTN: DRXBR-BM, J. Mester

DEPARTMENT OF THE NAVY

Chief of Naval Research
ATTN: Code 464, Jacob L. Warner
ATTN: Code 464, Thomas P. Quinn

Commander
Naval Air Systems Command
ATTN: AIR 5381

Commander
Naval Electronic Systems Command
ATTN: John E. DonCarlos
ATTN: PME 117-T, Satellite Comm. Project Off.
ATTN: NAVALEX 034, T. Barry Hughes
ATTN: PME 117

Commander
Naval Electronics Laboratory Center
ATTN: William F. Moler
ATTN: Code 0230, C. Baggett
ATTN: R. Eastman
3 cy ATTN: 2200

Commanding Officer
Naval Intelligence Support Ctr.
ATTN: Mr. Dubbin, STIC 12

Director
Naval Research Laboratory
ATTN: Hdq. Comm. Dir., Bruce Wald
ATTN: Code 5430
ATTN: Code 7700, Timothy P. Coffey
ATTN: Code 5460, Radio Electromag. Prop. Br.
3 cy ATTN: Code 7701, Jack D. Brown

Commander
Naval Space Surveillance System
ATTN: CAPT J. H. Burton

Commander
Naval Surface Weapons Center
ATTN: Code WA501, Navy Nuc. Prgms. Off.

Director
Strategic Systems Project Office
ATTN: NSP-2141

DEPARTMENT OF THE AIR FORCE

Commander
ADC/DC
ATTN: DC, Mr. Long

Commander
ADCOM/XPD
ATTN: XPQDQ

AF Geophysics Laboratory, AFSC
ATTN: SUOL, AFCRL Rsch. Lib.
ATTN: OPR, James C. Ulwick
ATTN: LKB, Kenneth S. W. Champion
ATTN: OPR, Alva T. Stair

AF Weapons Laboratory, AFSC
ATTN: SUL
ATTN: DYT, Capt L. Wittwer
ATTN: SAS, John M. Kamm

DEPARTMENT OF THE AIR FORCE (Continued)

AFTAC
ATTN: TF/Maj Wiley
ATTN: TN

Air Force Avionics Laboratory, AFSC
ATTN: AAD, Wade Hunt
ATTN: AFAL, AAB, H. M. Hartman

Headquarters
Electronic Systems Division, AFSC
ATTN: YSEV
ATTN: XRE, Lt Michaels
ATTN: Capt Rodrigues
ATTN: Lt Col J. Morin, CDEF XRC

Commander
Foreign Technology Division, AFSC
ATTN: TD-BTA, Library

HQ USAF/RD
ATTN: RDQ

Commander
Rome Air Development Center, AFSC
ATTN: EMTLD, Doc. Lib.

SAMSO/SZ
ATTN: SZJ, Maj Lawrence Doan

Commander in Chief
Strategic Air Command
ATTN: XPFS, Maj Brian G. Stephan

ENERGY RESEARCH AND DEVELOPMENT ADMINISTRATION

University of California
Lawrence Livermore Laboratory
ATTN: Tech. Info. Dept., L-3

Los Alamos Scientific Laboratory
ATTN: Doc. Con. for R. F. Taschek

Sandia Laboratories
ATTN: Doc. Con. for J. P. Martin, Org. 1732
ATTN: Doc. Con. for A. Dean Thornbrough
ATTN: Doc. Con. for W. D. Brown
ATTN: Doc. Con. for D. A. Dahlgren, Org. 1722

OTHER GOVERNMENT AGENCIES

Department of Commerce
Office of Telecommunications
ATTN: L. A. Berry
ATTN: William F. Utlaut
ATTN: G. Reed

National Oceanic & Atmospheric Admin.
Environmental Research Laboratories
ATTN: C. L. Rufenach
ATTN: Joseph H. Pope

DEPARTMENT OF DEFENSE CONTRACTORS

Aeronutronic Ford Corporation
Western Development Laboratories Div.
ATTN: J. T. Mattingley, M.S. X22

DEPARTMENT OF DEFENSE CONTRACTORS (Continued)

Aerospace Corporation
ATTN: T. M. Salmi
ATTN: V. Josephson
ATTN: SMFA for PWW
ATTN: Irving M. Garfunkel
ATTN: S. P. Bower

Analytical Systems Engineering Corp.
ATTN: Radio Sciences

The Boeing Company
ATTN: D. Murray
ATTN: Glen Keister

University of California at San Diego
ATTN: Henry G. Booker

Calspan Corporation
ATTN: Romeo A. Deliberis

Computer Sciences Corporation
ATTN: John Spoor
ATTN: H. Blank

Comsat Laboratories
ATTN: R. R. Taur

Cornell University
Department of Electrical Engineering
ATTN: D. T. Farley, Jr.

ESL, Inc.
ATTN: V. L. Mower
ATTN: R. K. Stevens
ATTN: James Marshall
ATTN: J. Roberts

General Electric Company
TEMPO-Center for Advanced Studies
ATTN: Don Chandler
ATTN: DASIAC
ATTN: B. Gambill

General Electric Company
ATTN: F. A. Reibert

General Research Corporation
ATTN: John Ise, Jr.

Geophysical Institute
ATTN: Neal Brown
ATTN: T. N. Davis
ATTN: Technical Library

GTE Sylvania, Inc.
ATTN: Marshal Cross

HRB-Singer, Inc.
ATTN: Larry Feathers

University of Illinois
Department of Electrical Engineering
ATTN: K. C. Yeh

Institute for Defense Analyses
ATTN: Joel Bengston
ATTN: Ernest Bauer
ATTN: J. M. Aein
ATTN: Hans Wolfhard

DEPARTMENT OF DEFENSE CONTRACTORS (Continued)

Intl. Tel. & Telegraph Corporation
ATTN: John M. Kelso

Intl. Tel. & Telegraph Corporation
ATTN: Tech. Lib.

Johns Hopkins University
Applied Physics Laboratory
ATTN: Document Librarian

Lockheed Missiles & Space Co., Inc.
ATTN: Dept. 60-12

Lockheed Missiles and Space Company
ATTN: Richard G. Johnson, Dept. 52-12
ATTN: Martin Walt, Dept. 52-10
ATTN: Billy M. McCormac, Dept 52-54

M.I.T. Lincoln Laboratory
ATTN: Mr. Walden, X113
ATTN: D. Clark
ATTN: James H. Pannell, L-246
ATTN: Lib. A-082 for David M. Towle

Martin Marietta Corporation
ATTN: Special Projects, Program 248

Maxwell Laboratories, Inc.
ATTN: Victor Fargo
ATTN: A. N. Rostocker
ATTN: A. J. Shannon

McDonnell Douglas Corporation
ATTN: J. Moule
ATTN: N. Harris

Mission Research Corporation
ATTN: R. Bogusch
ATTN: M. Scheibe
ATTN: Steven L. Gutsche
ATTN: P. Fischer
ATTN: R. Hendrick
ATTN: Dave Sowle

The Mitre Corporation
ATTN: S. A. Morin
ATTN: C. E. Callahan
ATTN: G. Harding
ATTN: J. C. Keenan
ATTN: Chief Scientist, W. Sen

The Mitre Corporation
ATTN: Allen Schneider

North Carolina State Univ. at Raleigh
ATTN: Sec. Officer for Walter A. Flood

Pacific-Sierra Research Corp.
ATTN: E. C. Field, Jr.

Photometrics, Inc.
ATTN: Irving L. Kofsky

Physical Dynamics, Inc.
ATTN: A. Thompson
ATTN: Joseph B. Workman

DEPARTMENT OF DEFENSE CONTRACTORS (Continued)

R & D Associates
ATTN: Robert E. Lelevier
ATTN: Richard Latter
ATTN: William B. Wright, Jr.
3 cy ATTN: Forrest Gilmore

The Rand Corporation
ATTN: Cullen Crain

Science Applications, Inc.
ATTN: D. Sachs
ATTN: E. A. Straker
ATTN: Lewis M. Linson

Science Applications, Inc.
ATTN: Dale H. Divis

DEPARTMENT OF DEFENSE CONTRACTORS (Continued)

Stanford Research Institute
ATTN: David A. Johnson
ATTN: Alan Burns
ATTN: E. J. Fremouw
ATTN: Walter Jaye
ATTN: Charles L. Rino
ATTN: Donald Neilson
ATTN: L. L. Cobb
ATTN: G. Smith
ATTN: Walter G. Chesnut
ATTN: Warren W. Berning

Systems Development Corporation
ATTN: E. G. Meyer

Tri-Com, Inc.
ATTN: Darrel Murray

TRW Systems Group
ATTN: Robert M. Webb, M.S. R1-1150
ATTN: R. K. Plebuch